AFRL-ML-WP-TR-2000-4154

EFFECT OF SURFACE PREPARATION ON FATIGUE DURABILITY OF BONDED COMPOSITE REPAIR PATCHES
VOLUME 6 – DELIVERY ORDER 4, TASK 1

D. Robert Askins
University of Dayton Research Institute
300 College Park Avenue
Dayton, OH 45469-0130

November 1999

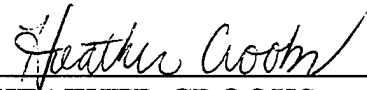**FINAL REPORT FOR PERIOD 01 MAY 1998 – 30 AUGUST 1999**

20020409 058

MATERIALS AND MANUFACTURING DIRECTORATE
AIR FORCE RESEARCH LABORATORY
AIR FORCE MATERIEL COMMAND
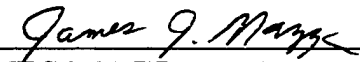WRIGHT-PATTERSON AIR FORCE BASE, OH 45433-7750

NOTICE

Using government drawings, specifications, or other data included in this document for any purpose other than government procurement does not in any way obligate the U.S. Government. The fact that the government formulated or supplied the drawings, specifications, or other data does not license the holder or any other person or corporation; or convey and rights or permission to manufacture, use, or sell any patented invention that may relate to them.

This technical report has been reviewed and is approved for publication.

This report is releasable to the National Technical Information Service (NTIS). At NTIS, it will be available to the general public, including foreign nations.

HEATHER CROOKS
Project Engineer
Adhesives, Comp & Elastomers Team
Materials Integrity Branch

JAMES MAZZA
Team Leader
Adhesives, Comp & Elastomers Team
Materials Integrity Branch

MICHAEL HITCHCOCK
Chief
Materials Integrity Branch
Manufacturing Technology Directorate

Copies of this report should not be returned unless return is required by security considerations, contractual obligations, or notice on a specific document.

REPORT DOCUMENTATION PAGE

Public reporting burden for this collection of information is estimated to average 1 hour per response, including the time for reviewing instructions, searching existing data sources, gathering and maintaining the data needed, and completing and reviewing this collection of information. Send comments regarding this burden estimate or any other aspect of this collection of information, including suggestions for reducing this burden to Washington Headquarters Services, Directorate for Information Operations and Reports, 1215 Jefferson Davis Highway, Suite 1204, Arlington, VA 22202-4302, and to the Office of Management and Budget, Paperwork Reduction Project (0704-0188), Washington, DC 20503

1. AGENCY USE ONLY (Leave blank)	2. REPORT DATE November 1999	3. REPORT TYPE AND DATES COVERED Final, 05/01/98 - 08/30/99

4. TITLE AND SUBTITLE

EFFECT OF SURFACE PREPARATION ON FATIGUE DURABILITY OF BONDED COMPOSITE REPAIR PATCHES

Volume 6 - Delivery Order 4, Task 1

5. FUNDING NUMBERS

C: F33615-95-D-5616
PE: 62102F
PR: 4349
TA: S2
WU: 00

6. AUTHOR(S)

D. Robert Askins

7. PERFORMING ORGANIZATION NAME(S) AND ADDRESS(ES)

University of Dayton Research Institute
300 College Park Avenue
Dayton, OH 45469-0130

8. PERFORMING ORGANIZATION REPORT NUMBER

UDR-TR-1999-00054

9. SPONSORING / MONITORING AGENCY NAME(S) AND ADDRESS(ES)

Materials and Manufacturing Directorate
Air Force Research Laboratory
Air Force Materiel Command
Wright-Patterson AFB, OH 45433-7750
POC: Heather Crooks, AFRL/MLSA, (937) 255-7484

10. SPONSORING / MONITORING AGENCY REPORT NUMBER

AFRL-ML-WP-TR-2000-4154

11. SUPPLEMENTARY NOTES

12a. DISTRIBUTION / AVAILABILITY STATEMENT

Approved for public release; distribution unlimited.

12b. DISTRIBUTION CODE

13. ABSTRACT *(Maximum 200 Words)*

A test program was conducted to investigate two issues:
(a) Whether fatigue testing could discriminate between optimum and inferior surface preparations.
(b) Whether a correlation exists between wedge and fatigue test results.

Wedge and fatigue specimens were prepared with two surface preparations. One was considered to be highly durable and one to have poor durability in hot-wet environments. The highly durable preparation involved a Grit-Blast Silane (GBS) surface treatment with BR127 primer. The poor durability preparation consisted of Scuff Sanding (SS) with no primer. The fatigue specimens consisted of an aluminum panel with a bonded boron/epoxy composite patch. The wedge specimens behaved as expected, with the GBS/BR127 surface preparation exhibiting low-crack growth and cohesive failure while the SS/no primer surface preparation exhibited high-crack growth and interfacial failure.

The fatigue performance was quantified by obtaining periodic C-scans during the tests and determining the percentage of the patch bond area that was degraded as fatigue cycling progressed.

Comparison of these C-scan results, as well as failure modes, with the wedge test results, indicated that there was relatively good correlation between wedge and fatigue behavior for the two extremes of surface preparation investigated here.

14. SUBJECT TERMS

Adhesive, Primer, Composite Patch, Repair, Surface Preparation, Aluminum, Grit-Blast Silane, Wedge, Fatigue, Hot-Wet, Environmental Aging, Failure Analysis, Durability, Life, Interface, Boron Composite, Epoxy

15. NUMBER OF PAGES

78

16. PRICE CODE

17. SECURITY CLASSIFICATION OF REPORT UNCLASSIFIED	18. SECURITY CLASSIFICATION OF THIS PAGE UNCLASSIFIED	19. SECURITY CLASSIFICATION OF ABSTRACT UNCLASSIFIED	20. LIMITATION OF ABSTRACT SAR

TABLE OF CONTENTS

TABLE OF CONTENTS (Concluded)

LIST OF TABLES

PREFACE

This report covers the work performed by the University of Dayton Research Institute (UDRI), Dayton, Ohio, during the period from May 1998 to August 1999. The work was conducted under Air Force Contract F33615-95-D-5616, Delivery Order 0004. The project was directed by Mr. James Mazza, Air Force Research Laboratory (AFRL/MLSA) of Wright-Patterson Air Force Base (WPAFB), Ohio. Mr. Bill Schweinberg (TIEDD) of Warner-Robins (WR-ALC), Georgia was the Air Force Project Engineer.

The work was performed at UDRI with Mr. D. R. Askins acting as the Principal Investigator. Specimen preparation, environmental exposure, and wedge testing were carried out by Mr. Gary Andrews. Messrs. Sam Macy, Trey Coleman, and Dave Allen conducted the fatigue testing. Additional contributions were made by Mr. Peter Muth.

This report was submitted for publication in November 1999. The contractor's report number is UDR-TR-1999-00054.

SECTION 1

INTRODUCTION

During the past decade, much developmental work has been carried out to provide aircraft maintenance personnel with the materials, processes and supporting data needed to confidently use bonded composite materials in the repair of damaged aluminum aircraft structure. As a result of this work, bonded composite repairs have become commonplace on many military aircraft.

The materials and processes used in aircraft repair must meet a different set of criteria than those used in original construction. One major difference is that the equipment and tooling available in manufacturing plants are not available in the field or at most depots. Since most repairs are carried out on the aircraft, the work environment imposes further constraints. A brief overview of some of these differences is briefly detailed in Table 1. Even though Table 1 indicates a variety of available heating sources for repair, there are some situations in which it is highly desirable to avoid the use of electrical power altogether. One such situation is inside an integral wing fuel tank. If a repair must be made inside such a fuel tank, the process becomes long and cumbersome because of the precautions that must be undertaken to eliminate the risk of explosion. For example, because the current curing methods are not considered to be intrinsically safe (possible arcing with the electrically powered equipment), the current C-141 Repair Technical Order (T. O.) requires that all fuel tanks must be totally drained, depuddled, and air purged. This, in turn, by Environmental Protection Agency (EPA) requirements, means that the work must be accomplished in a fuel barn [Ref. 1]. Further, the need to apply heat at various stages of the repair process requires a variety of heating equipment and a higher skill level on the part of the maintenance personnel.

Table 1. Typical Differences Between Original Manufacturing and Repair Environments

Item	Original Manufacturing Environment	Repair Environment
Surface Preparation	Large acid and rinse tanks, Grit blasting in large booth,	No acids allowed or must be specially contained, Grit blasting not desired in some locations (inside fuel tanks)
Primer Curing	Oven	Heat lamps
Adhesive Curing	Autoclave, Oven	Heat blanket, Heat lamps, Forced hot air blowers
Pressure Source	Autoclave, Vacuum bag	Vacuum bag, Clamps

One of the procedures currently being used for on-aircraft repair with bonded composite patches is a grit-blast silane (GBS) surface preparation process. This process does not

require the use of acids and has been demonstrated, through extensive laboratory testing, to produce aluminum-to-aluminum adhesive bonds that have excellent resistance to environmental degradation. The laboratory work that has demonstrated the environmental durability of this prebond surface treatment process has primarily relied on the use of the wedge crack-propagation test (ASTM D 3762). While this test is generally considered to be an excellent means of evaluating the relative environmental durability of different surface preparation procedures, it does not provide a direct indication of "how good is good enough." Further, the relationship between wedge crack-propagation results on aluminum-to-aluminum specimens and fatigue test results on panels with bonded composite patches over cracked aluminum substrate panels has not been documented. This latter type test more realistically simulates repaired aircraft structure and the type of loading to which it is subjected than the wedge specimen.

The factors cited above provided the impetus for the investigation described in this report. Guided by the desire to simplify maintenance procedures and reduce the time needed to carry them out without compromising the quality of bonded repairs, there were two objectives:

(a) To determine whether fatigue testing could discriminate between optimum and inferior surface preparations.

(b) To determine whether a correlation exists between wedge and fatigue test results.

SECTION 2

APPROACH

Test specimens were prepared, using surface processing conditions known from wedge tests to produce optimum and inferior environmental durability. The primary interest was in generating data on the environmental durability of composite patches adhesively bonded to aluminum substrates. The composite patch material, the aluminum substrate material, and the bonding materials used were those actually used in the on-aircraft repair of cracked structure. The surface preparation processes comprised the experimental variables in the study.

Table 2 identifies the two different surface preparation processes that were used and lists the particular processing conditions for each that were used or varied to achieve the optimum or inferior condition. Further details of these surface preparations are discussed in Section 3. The surface preparation procedures listed in Table 2 were selected because it was believed that they would bracket the behavior of surface preparations that might ultimately be of interest. They represent what are felt to be the best- and worst-case surface preparations that might be used in on-aircraft repair. This approach was adopted to determine whether a correlation between wedge and fatigue results could be discerned for the extreme best and worst surface preparation cases. If a correlation could be established for these extremes, then the intermediate cases, in which the surface treatment would be expected to produce an environmental durability between the best and worst cases listed in Table 2, can be investigated.

Table 2. Optimum and Inferior Surface Preparation Procedures

OPTIMUM	INFERIOR
GBS/BR127 (1)	Scuff-Sand (2)
• 200 °F Silane Drying • 250 °F Primer Curing	• No silane used • No primer used

(1) GBS surface preparation procedure is described in Reference 2.
    All GBS specimens were primed with BR127.
(2) Scuff-Sand (SS) surface preparation procedure is described in Appendix D.
    No primer was used on SS specimens.

Two types of test specimens were employed. These were wedge crack-propagation (ASTM D 3762) and fatigue. The former test is widely acknowledged to be an excellent means of discriminating between environmentally durable and nondurable surface preparations. Since this test utilizes a metal-to-metal bond, it does not provide a direct indication of the performance of a composite-to-metal bond. The other problem with this test is that no definitive criteria has been established that defines what level of performance is good enough for any particular application. A fatigue test that employs a metal panel bonded to a composite patch is believed by many engineers to be the most

3

realistic simulation of an actual repaired piece of aircraft structure. No previous correlation between the performance of wedge and fatigue test specimens had been established. As a consequence, one of the objectives of this investigation was to perform both of these tests on specimens prepared with the same materials and processes to determine whether such a correlation exists.

The test matrix shown in Table 3 was jointly agreed to by WR-ALC/TIEDD and AFRL/MLSA and was carried out on specimens prepared with both of the surface preparation procedures listed in Table 2. Further details of the particular test parameters and procedures are discussed in Section 4. The test conditions listed in Table 3 were determined by WR-ALC/TIEDD to be realistic for the applications of interest to them. The wedge specimens were in accordance with the ASTM test standards cited above. The fatigue specimen design was determined by WR-ALC to be a realistic simulation of the repair situations they were interested in. The detailed designs of the fatigue specimen and repair patch are described in Sections 3.1 and 3.2.

Table 3. Test Matrix to Characterize Optimum and Inferior Bonded Joints

Test Type	No. of Specimens for Each Surface Preparation (1)		
	72 °F, Unaged	72 °F, Aged (2)	120 °F, Aged (2)
Wedge	-----	-----	2 panels, 5 spec. each
Fatigue (R=0.1)	5	5	1
Fatigue (R=0.5)	1	1	1

(1) Two surface preparations were tested: GBS and SS. The former is known to be a durable surface preparation that is expected to perform well in both tests. The latter is considered to be an inferior surface preparation that was not expected to perform well in either test.

The total number of specimens to be tested is:
   Wedge -   10 per surface prep., 20 total
   Fatigue -   14 per surface prep., 28 total

The following abbreviations are used in this report for the three test conditions listed here.
   RTD (room temperature dry) = 72 °F, Unaged
   RTW (room temperature wet) = 72 °F, Aged
   120W (120 °F, wet) = 120 F, Aged

(2) Aged: Fatigue specimens were tested at 120°F after aging in a 160 °F, 95-100%RH environment for a minimum of 84 days (12 weeks) prior to testing. Wedge specimens were tested in a 120 °F, 95-100%RH environment with no prior aging.

SECTION 3

MATERIALS AND PROCESSES

As noted previously, there were a number of material and process variables incorporated into this investigation. These as well as the detailed design of the fatigue specimen and repair patch are described in the following sections.

3.1   ALUMINUM SUBSTRATE PANELS

All of the various types of specimens used in this investigation were prepared with 7075T6 bare aluminum. The wedge specimens were made in accordance with ASTM D3762. The fatigue specimens consisted of 3.17-mm (0.125-inch) thick aluminum machined to the design illustrated in Figure 1. As illustrated in Figure 1, 1.6-mm (0.063-inch) doubler tabs were bonded to each end of the aluminum panels to lessen the effect of stress concentration around the boltholes. The ends of each test panel were bolted between 23-mm (0.9-inch) thick loading plates with a bolt torque of 20 ft-lb (27.1 N-m). The loading plates were pin-mounted in the fatigue test machine.

3.2   COMPOSITE REPAIR PATCHES

All of the repair patches were made with 5521/4 boron/epoxy (B/Ep) prepreg. This is made by Textron Specialty Materials but was supplied for this effort by WR-ALC.

The repair patches were made by cutting plies from 6-inch wide B/Ep prepreg using a razor knife. Each ply was cut to the required length and width and hand-laid-up to achieve the required number of plies and ply drop-off distances at the ends of the patch. The patches were laid-up with their faying surface on a resin-rich peel-ply (E761/ 52006 by Fiber Cote). This was left on the patch until the patch was to be bonded. Each patch was cured in an autoclave using a cure cycle recommended by Textron. The cure schedule was as follows:

- Apply full vacuum and apply 50 psi positive pressure,
- Heat at a rate of 5 °F/min (2.8 °C/min),
- When the temperature reaches 235 °F(113 °C), release the vacuum,
- When the temperature reaches 250 °F (121 °C), hold at that temperature for 60 minutes,
- Cool at 5 °F (2.8 °C)/min,
- When the temperature reaches 120 °F(49 °C) release the pressure and remove the composite patch from the autoclave.

The plies were all oriented unidirectionally so as to align with the load direction in the fatigue specimen. All of the patches were rectangular and were 11 plies thick,

6

15 hole pattern
for gripping
(0.25" dia.)

34

6

0.75

0.75

0.325

0.75

1.0

* All units in inches

Figure 1. Aluminum Fatigue Specimen Design

69.9 mm (2.75 inches) wide, and 150 mm (5.9 inches) long and consisted of an inverted wedding cake layup, as illustrated in Figure 2. This width provided a patch that left a free distance of 41.3 mm (1.625 inches) on each side of the patch between edges of the patch and the edges of the aluminum panel. There was also a free distance of 311 mm (12.25 inches) between the end of the patch and the end of the gage section (first row of loading boltholes). This distance is slightly over two times the length of the patch, so that the entire gage section is just over five times the length of the patch. Figure 3 illustrates the patch on the substrate panel.

The 11-ply patch thickness was dictated by the desire to achieve a composite patch-to-aluminum stiffness ratio of 1.2. Appendix A.1 presents the calculations leading to this patch thickness and explains how the final stiffness ratio actually was 1.23 rather than 1.2. The overall patch length was dictated by a number of requirements. These were specified by WR-ALC/TIEDD and included the following:

- The patch-to-aluminum stiffness ratio was to be 1.2,
- The taper (ply drop-off) rate on each end of the patch was to be 10:1, and
- The total length of the composite patch was to be determined according to a modification of the procedure outlined by Baker [Ref. 3].

The detailed calculations, based on the requirements noted above, that led to the final overall patch length, are presented in Appendix A.2. These calculations explain why the final overall patch length was fixed at 5.9 inches.

It should be noted that there were two exceptions to normal patch design practice. First as illustrated in Figure 2, there was a 1.27-mm (0.05-inch) drop off for each ply on each end of the patch. This corresponds to an end taper of 6° (10:1 ratio of drop-off length to ply thickness) and is considerably more abrupt than is generally recommended (30:1 or ~2°). This abrupt ply drop-off rate was used to magnify the peel stresses at the ends of the patch. This would place a more severe demand on the bond strength and on the resistance of the bond to environmental attack. It was felt that this would enhance the discrimination between the "good" and "inferior" surface preparations. Second, the length of the constant thickness portion of the patch was double the length suggested by Baker ($12/\beta$ rather than $6/\beta$). Both of these exceptions were specified by WR-ALC/TIEDD as a means of increasing the likelihood of a debonding failure along the bondline.

A peel ply was left on the faying surface of each patch for removal just prior to bonding to preserve an uncontaminated bonding surface. When the composite patch was ready to be bonded to the cracked aluminum substrate panels, the peel ply was removed from the composite faying surface.

Ply No.
11
10
9
8
7
6
5
4
3
2
1

Length
(inches)
5.9
5.8
5.7
5.6
5.5
5.4
5.3
5.2
5.1
5.0
4.9

₵

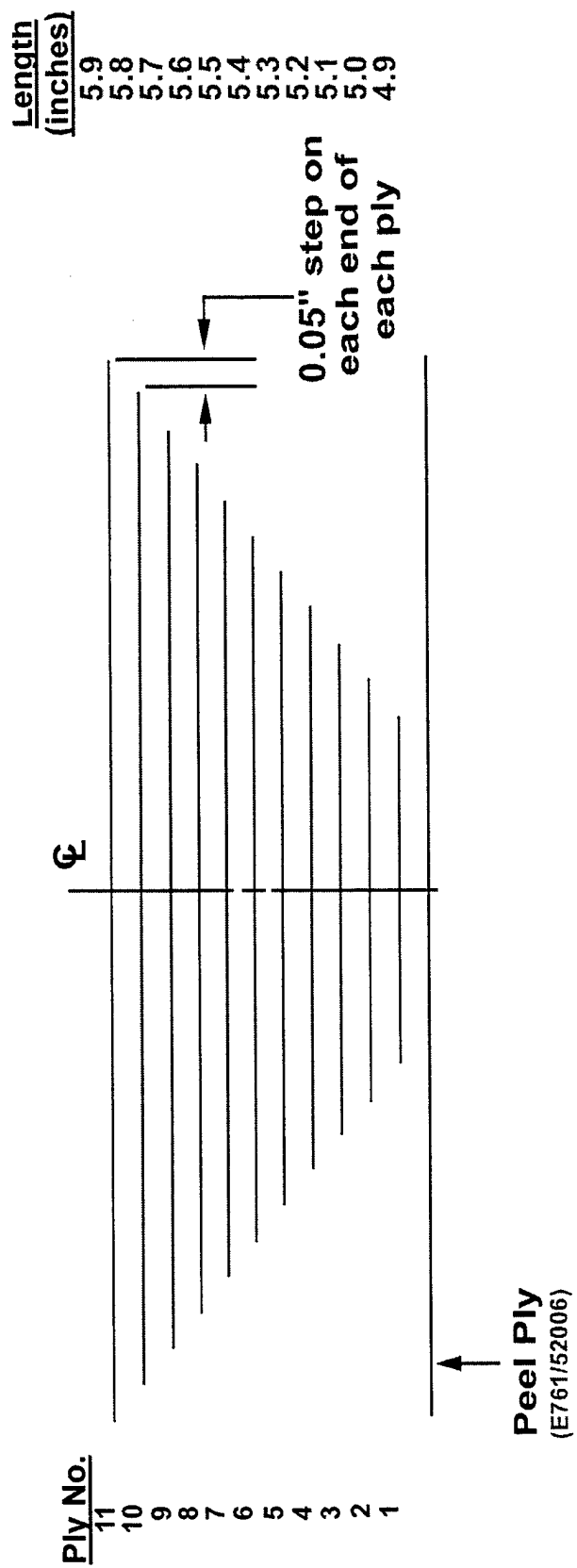0.05" step on
each end of
each ply

Peel Ply
(E761/52006)

Figure 2. Longitudinal Cross-Section of Boron/Epoxy Composite Patch

9
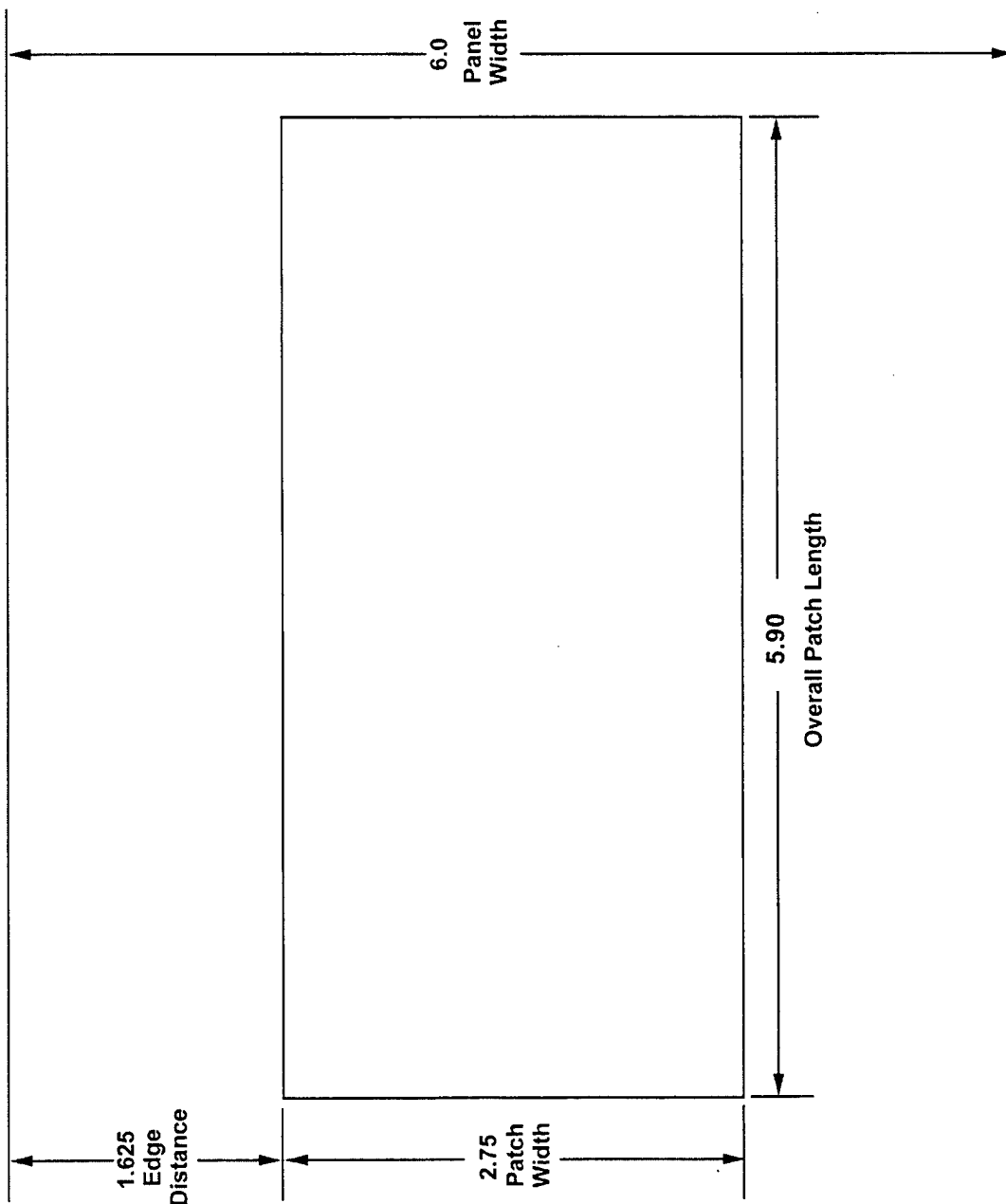
Figure 3. Positioning of Composite Patch on Aluminum Substrate Panel

6.0
Panel
Width

5.90

Overall Patch Length

1.625
Edge
Distance

2.75
Patch
Width

3.3 SURFACE PREPARATIONS

As noted in Table 2, two different aluminum surface preparations were used in the preparation of the test specimens listed in Table 3. One of these, GBS, was known to produce environmentally durable bonding surfaces and was designated as the optimum surface preparation.

The GBS surface treatment was originally developed by the Australian Aeronautical Research Laboratory. The process does not employ hazardous chemicals or complicated equipment. Subsequent work conducted by UDRI under Air Force sponsorship was crucial in identifying the process variables that were critical in achieving consistent, high quality surface treatments. This latter work also established how much the critical process variables could be varied without compromising the quality of the finished surface. A UDRI technical report, UDR-TR-94-153 [Ref. 4], details the approach, procedures, and results of the investigation and provides a recipe for the optimum GBS procedure. The environmental durability of prebond aluminum surfaces prepared by the GBS process has been demonstrated to be excellent.

The other aluminum surface preparation used in the program was a simple scuff-sanding process with no silane and no primer. The scuff-sand procedure consists of two steps. First, the surface of the aluminum is scrubbed with a Scotch-Brite pad (blue) and methyethylketone (MEK) until it looks like a polished surface. Second, the scrubbed surface is thoroughly cleaned with reagent grade MEK and unpigmented/unscented tissues (i.e., KimWipes) by wiping from center to edge of the surface until no contamination (black marks or streaks) is evident on the tissues. Following this, the adhesive was applied as described in Section 3.5. It was recognized that this would probably produce a surface that was markedly inferior to that achievable with the GBS treatment. Nevertheless, this inferior treatment was used to provide a worst-case contrast to the best-case GBS treatment. As described in Section 2, this would serve to bracket the durability performance and provide a set of extreme cases with which to determine whether a correlation exists between wedge crack-propagation and fatigue test results.

The surface preparations described above were applied to the entire width of the aluminum panels and to a portion of the panel midsections that extended 102 mm (4 inches) on either side of the center crack (a total prepared area of 152 by 203 mm (6 by 8 inches).

3.4 ADHESIVE PRIMER

The GBS surface preparation was followed by the spray application of BR127 corrosion inhibiting adhesive primer over the 152 by 203 mm (6 by 8 inches) prepared area. This primer was applied within one hour after completion of the surface preparation to a thickness of 0.0025-0.0760 mm (0.0001-0.0003 inch). After application, the primer was

air-dried at 22 °C (72 °F) for 30 minutes followed by an oven-bake cycle of 60 minutes at 121 °C (250 °F) to cure the polymer in the primer. After curing of the primer, the application of the adhesive and the bonding cycle can be delayed for up to several weeks so long as the primed surfaces are kept protected from damage and in a reasonable room temperature and humidity environment. In the preparation of the specimens in this program, there was minimal delay between priming and bonding. Generally, the adhesive application and bonding cycle were carried out the same or next day after primer application and cure.

The final primer thickness was measured with a Fisher Isoscope MP2 eddy current instrument and corroborated visually by comparison of the primed test specimen with color chips of certified primer thickness from the primer manufacturer.

3.5   ADHESIVE AND PANEL BONDING

All of the specimens were bonded with one ply of 415g/m² (0.085lb/ft²) AF163-2 epoxy film adhesive. This adhesive is manufactured by 3M. The bonding cycle was carried out in a circulating air oven and consisted of 1 hour at 121 °C (250 °F) in a vacuum bag at 355-406 mm (14-16 inches) Hg vacuum. No effort was made to constrain the thermal expansion or contraction of the panel components during the bonding cycle. Since the thermal expansion coefficients of the aluminum substrate panels and composite patches are different, the fatigue panels exhibited slight curvature after bonding. Consideration was given to attempting to constrain the fatigue panels during bonding but it was decided not to do so. Appendix B explains the rationale for permitting free expansion and contraction during bonding.

When a composite patch was to be bonded to an aluminum substrate panel, the peel-ply on the faying surface of the patch was peeled off. This presented a clean composite surface to the adhesive. The preparation of the aluminum surfaces for bonding was discussed in Section 3.3.

SECTION 4

## TEST PROCEDURES

4.1 NONDESTRUCTIVE INSPECTION (NDI)

Each fatigue panel was nondestructively inspected before fatigue testing was started in order to establish the initial quality of the specimen. The inspections consisted of a through-transmission ultrasonic C-scan in a water-filled inspection tank. Figure 4 illustrates the NDI setup. A specimen was mounted 0.75 inch above and parallel to a flat glass reflector plate with the composite patch facing up. A 1/2-inch, 5-MHz transducer with a 3-inch focus was positioned 3 inches from the upper surface of the specimen. The ultrasonic energy from the transducer passed down through the specimen, was reflected from the reflector plate, passed back up through the specimen, and returned to the transducer. The patched region of the fatigue specimen was traversed by the transducer along a series of parallel longitudinal paths 0.016 inch apart. The mechanical traversing system had 0.001-inch position resolution.

The sensitivity of the inspection system was calibrated using a signal that passed through only the aluminum component of the specimen and reflected off the glass reflector plate. The gain of the ultrasonic instrument was initially adjusted to set the amplitude of the reflected signal to 100 percent of the vertical range of the instrument display. The instrument gain was then increased by 9 dB, an amount empirically determined to provide a 100 percent reflected signal for sound that passed through a patch and the aluminum substrate that were considered to be bonded well. An electronic gate was set to measure the amplitude of the reflected signal. With this calibration, reductions in amplitude indicate attenuation due to variations in bond integrity, assuming uniform and unchanging quality of the patch and the aluminum substrate.

The gated amplitude data was converted with a color palette into a C-scan (plan-view) display of the attenuation of the patched area of the specimen. Dark blue represents high attenuation (low level of signal return), white represents low attenuation (high level of signal return), and other colors represent intermediate attenuations. Expressed in percentages, the attenuation range for each color is as follows:

White	0-7%	Yellow	52-58%
Pink	8-13%	Yellow Green	59-64%
Red	14-20%	Green	65-70%
Purple	21-26%	Dark Green	71-77%
Dark Red	27-32%	Light Blue	78-83%
Brown	33-39%	Medium Blue	84-89%
Orange	40-45%	Blue	90-96%
Yellow Orange	46-51%	Dark Blue	97-100%

Black would indicate no data taken, e.g., due to a rough specimen surface.

13
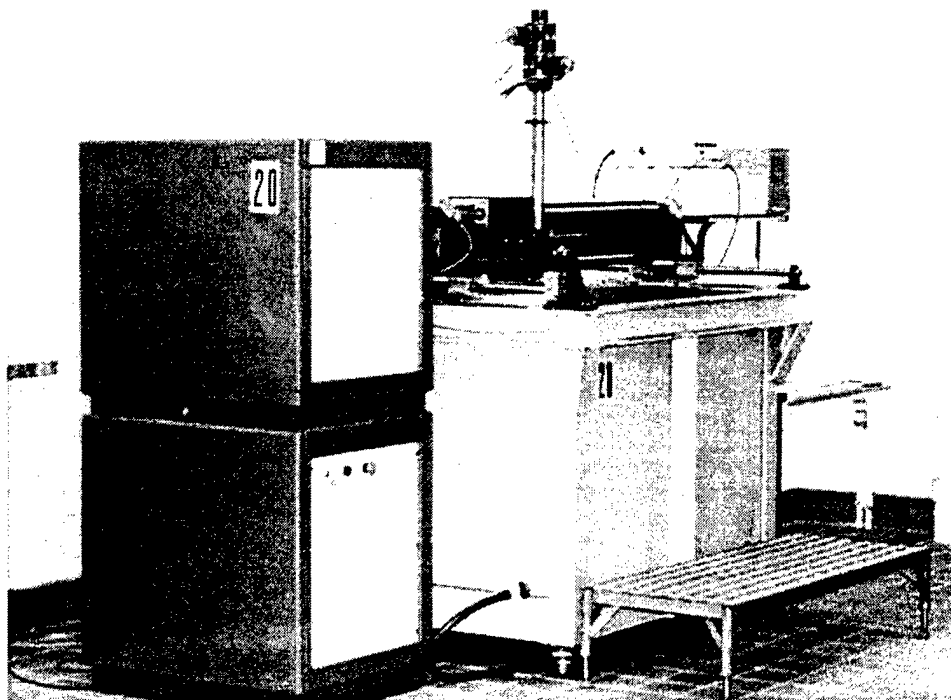
(a) Immersion Tank and C-Scanning System
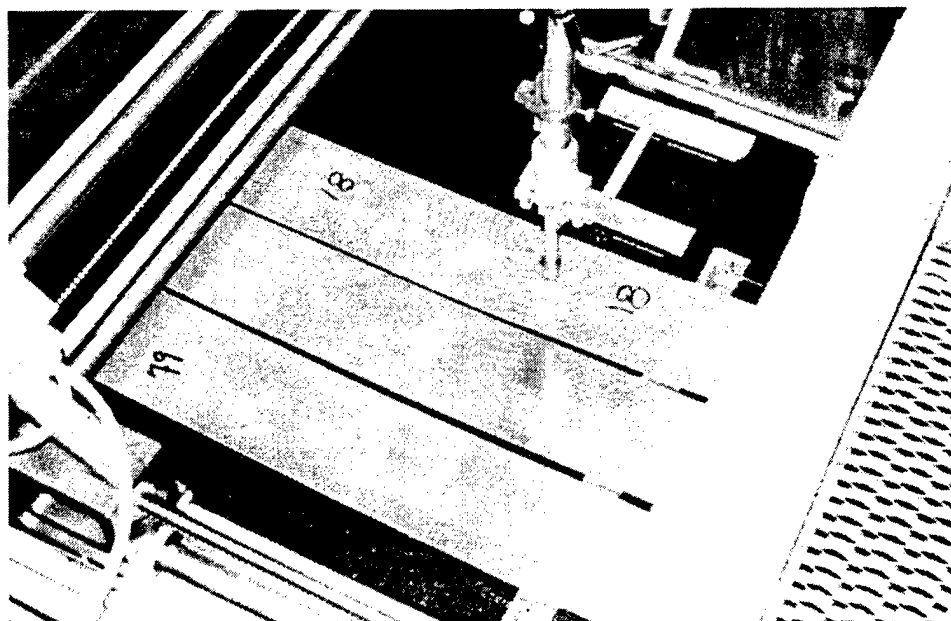
(b) C-Scanning of Three Specimens (Patches on Underside)

Figure 4. Nondestructive Inspection System Setup for Patched Specimens

Since this report is limited to black/white/shades-of-gray presentation, the colors listed were converted to shades-of-gray for purposes of illustrating the C-scans. The intermediate and higher levels of attenuation that were detected in some areas of the composite patches in the initial pretest C-scans are attributable to a variety of causes. The principal causes include the adhesive-rich flow areas around the periphery, porosity in the bondline, and the geometric effects of the taper (ply drop-offs) on the ends of the patches. The taper and the resin-rich flow areas cause attenuation by reflecting or refracting the ultrasonic signals at oblique angles while the porosity causes attenuation by scattering the signal as it encounters voids in its passage through the patched area.

4.2 STRAIN SURVEY ON PATCHED ALUMINUM SUBSTRATE PANEL

One of the concerns going into this test effort was whether the stress concentration at the ends of the patches would be high enough to cause premature panel failure during fatigue cycling since the applied fatigue loads would be quite high. Two specimens of each surface preparation were instrumented with five strain gages to measure panel strains in various locations. Figure 5 illustrates the gage locations.

The load-strain behavior at each gage location was recorded for each of the four instrumented panels in its initial condition and again periodically during its load-cycling. The strain data for each location and surface preparation was correlated with a number of load-cycles and was also compared to the predicted stress-concentrations obtained by WR-ALC via a finite element analytical technique.

4.3 ENVIRONMENTAL EXPOSURE

As indicated in Table 3, some of the fatigue specimens were environmentally aged before they were tested. The wedge crack propagation specimens were not aged prior to testing since the nature of this test is that the specimens go directly into the test environment (49°C/120°F and 95-100%RH) at the start of the test. The aging of the fatigue specimens was carried out in a humidity cabinet at 71°C (160°F) and 95-100%RH. Although the duration of the exposure varied depending on test machine availability, the fatigue specimens were all aged for a minimum of 154 days.

When the fatigue specimens had completed pretest aging, they were removed from the humidity cabinet and sealed in a moisture-proof bag with wet paper towels enclosed to prevent dryout. When the specimens were mounted in the test machine, the gage section was enclosed in a sealed bag with a wet towel inside to maintain a wet environment during the test.

The length of time that the fatigue specimens needed to be aged prior to testing was based on data generated during a previous lab investigation of moisture diffusion into a specimen of the type used here. In that study, an embedded moisture sensor in a dummy

15
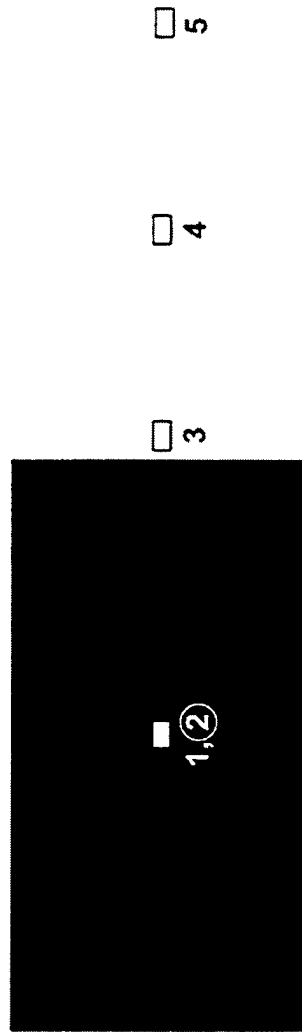
Gage Number	Location
1	Center of Patch
2	Bottom of Panel, Directly Under #1
3	Within 1/8" of End of Patch
4	2" from End of Patch
5	6" from End of Patch
	Gages 1,3,4,5 all on patched side of panel. Gage 2 on underside of panel.

Figure 5. Strain Gage Locations on Strain Survey Specimens

specimen was utilized to determine how long would be required for the center of the bondline to reach moisture equilibrium. An electrical resistance sensor, 0.13-mm (0.005-inch) thick, 12.7-mm (0.5-inch) wide, and 25.4-mm (1-inch) long, was embedded in a dummy sample to track moisture pickup. The sensor resistance changes as the moisture content of the environment changes. By aging a sample with an embedded sensor until the resistance stops decreasing and levels off, one can determine how long it takes for the sample to reach an equilibrium moisture condition. While this does not necessarily provide a quantifiable measure of the actual moisture content, it does indicate how long it takes for the moisture content to equilibrate.

The dummy sample consisted of a 12-ply B/Ep composite bonded to a piece of 7075T6 aluminum with a sensor embedded in the FM73M adhesive (415 g/m^2; 0.085 lb/ft^2) bondline. Figure 6 schematically illustrates this dummy sample. It was assumed that since the dimensions of the dummy sample illustrated in Figure 6 were nearly the same as the patch dimensions on the fatigue panels used in this study, the results from this previous study would be applicable.

The dummy moisture pickup sample described above was aged in a humidity cabinet at 71 °C (160 °F), 95-100 %RH. The electrical resistance of the sensor embedded in the dummy sample is illustrated in Figure 7. During the time segment labeled A, the sample was absorbing moisture. During the segments labeled B and C, the sample was losing moisture. It is evident from Figure 7 that a patched specimen loses absorbed moisture very slowly, even when it is openly exposed to ambient laboratory conditions.

4.4   WEDGE CRACK-PROPAGATION TESTS

The wedge crack-propagation test has been shown to be an excellent means of discriminating between environmentally durable and nondurable prebond surface treatments. The test method is fully described in ASTM D 3762 and the reader is referred to that document for the specimen and test details.

In this program, the wedge tests were carried out in a 49 °C (120 °F), 95-100 %RH environment and both the crack propagation rate and failure modes are reported.

4.5   FATIGUE TESTS

The fatigue tests performed in this effort were not governed by a specific test specification (such as ASTM) that can be referenced. The specimen design and test procedures were selected based on extensive prior experience with these test and specimen types and on the extensive body of fatigue test work involving cracked aluminum panels repaired with composite patches reported in the literature. Reference 4 provides a good summary of the published literature in this subject area. Figure 3 in Section 3.2 illustrates the fatigue specimen with the composite patch bonded in the center.

Aluminum Plate
102 mm X 229 mm

B/Ep Patch
(Bonded to Al Plate)
70 mm X 146 mm

Electrical Resistance Sensor
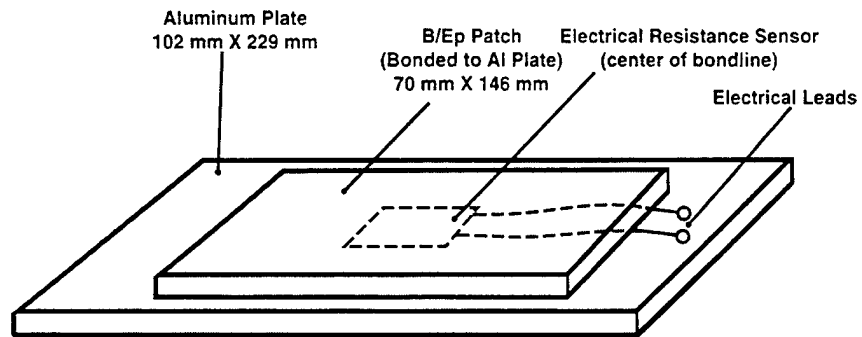(center of bondline)

Electrical Leads

Figure 6. Moisture Sensor Embedded in Bondline Between B/Ep Patch and Aluminum Plate
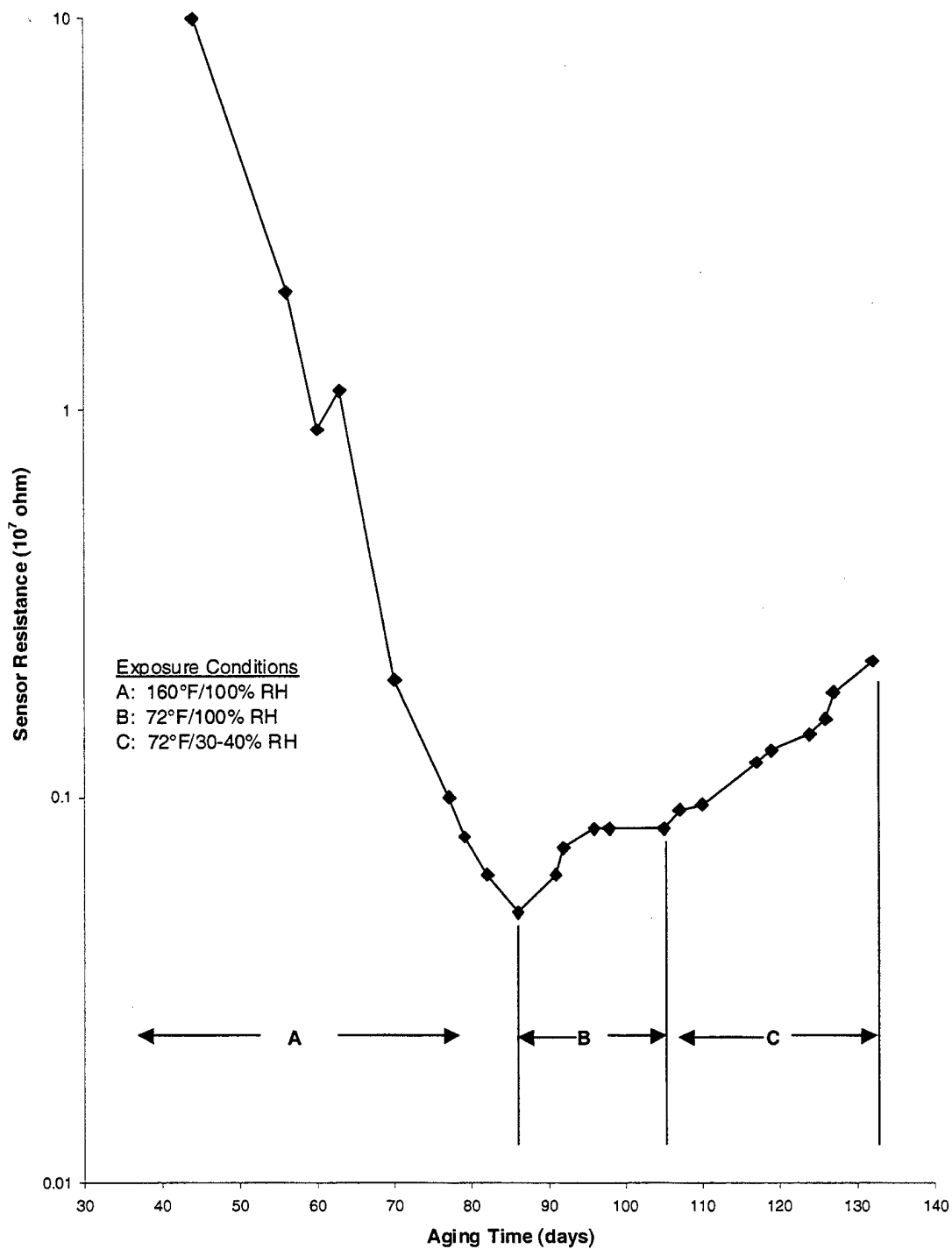
Figure 7. Effect of Humidity Aging on the Resistance of a Sensor Embedded in the Bondline of a Patched Panel

The fatigue tests consisted of constant amplitude, tension-tension loading, at a frequency of 1 Hz, with a minimum/maximum stress ratio of either 0.1 or 0.5. The maximum stress in each test was 276 MPa (40,000 psi) and the minimum stress was either 27.6 or 138 MPa (4,000 or 20,000 psi). Table 3 in Section 2 lists the test matrix for each surface preparation investigated during this program. The three test conditions were 22 °C (72 °F) on specimens that were not humidity-aged and 22 and 49 °C (72 and 120 °F) on specimens that had been humidity-aged at 71 °C (160 °F) and 95-100 %RH for at least 22 weeks. Figure 8 illustrates a 120 °F test specimen mounted in the fatigue machine.

Since the fatigue specimens did not contain precracks, there was no crack-growth measurement by which to track test progress. The primary concern during these tests was whether the patches debonded from the aluminum panels as a result of the load-cycling and, if so, at what point and to what extent. Two approaches were utilized to detect this.

First, visual observations were recorded during each test. The test technician looked to see if cracks appeared around the edges of the patch and if portions of the patch appeared to be sliding over the substrate panel during each load cycle. Second, each test was periodically interrupted to obtain a C-scan of the patch area. Changes in the signal attenuation through the patch, bondline, and aluminum would result if either the patch delaminated or became disbonded from the aluminum panel. These C-scans were used as a measure of both initial as well as residual "bondline integrity." The "bondline integrity" was arbitrarily defined to be good if over 50% of the transmitted ultrasonic signal was received back. The reason for using this as a criteria for good bondline integrity is that nearly all of the bond area on the panels exceeded this signal transmission level prior to the start of fatigue cycling.

Special care was taken on the tests that involved humidity-aged specimens to prevent dry out during the test. Immediately upon removal from the humidity chamber, these specimens were sealed in an aluminum foil bag with a wet paper towel inside. When these specimens were mounted in the test machine, an aluminum foil envelope 133 by 305 mm (5.25 by 12 inches) was taped over the composite patch with a wet paper towel covering the patch within the foil bag. This kept the patch and bondline in a 100 %RH environment until the test was concluded. When C-scans were obtained, the specimen was removed from the test machine with the wet bag enclosing the patch intact. The wet bag was left on the specimen until it was placed in the inspection tank and it was replaced on the specimen as soon as the C-scan was completed. Thus, the patch and bondline region never had an opportunity to dry out. The time lapse from when the specimen was removed from the test machine until it was returned to the test machine after C-scanning typically ranged from overnight to a few days. Dry-out measurements with the dummy specimen described in Section 4.3 are illustrated in Figure 7. This data indicates that exposure of a saturated specimen to ambient laboratory conditions for 2 weeks resulted in only a minor loss of absorbed moisture from the bondline. Because of this very slow rate of moisture loss, we are confident that keeping the specimen in a wet bag preserves its moisture content after removal from the humidity cabinet and during the C-scan interruptions.
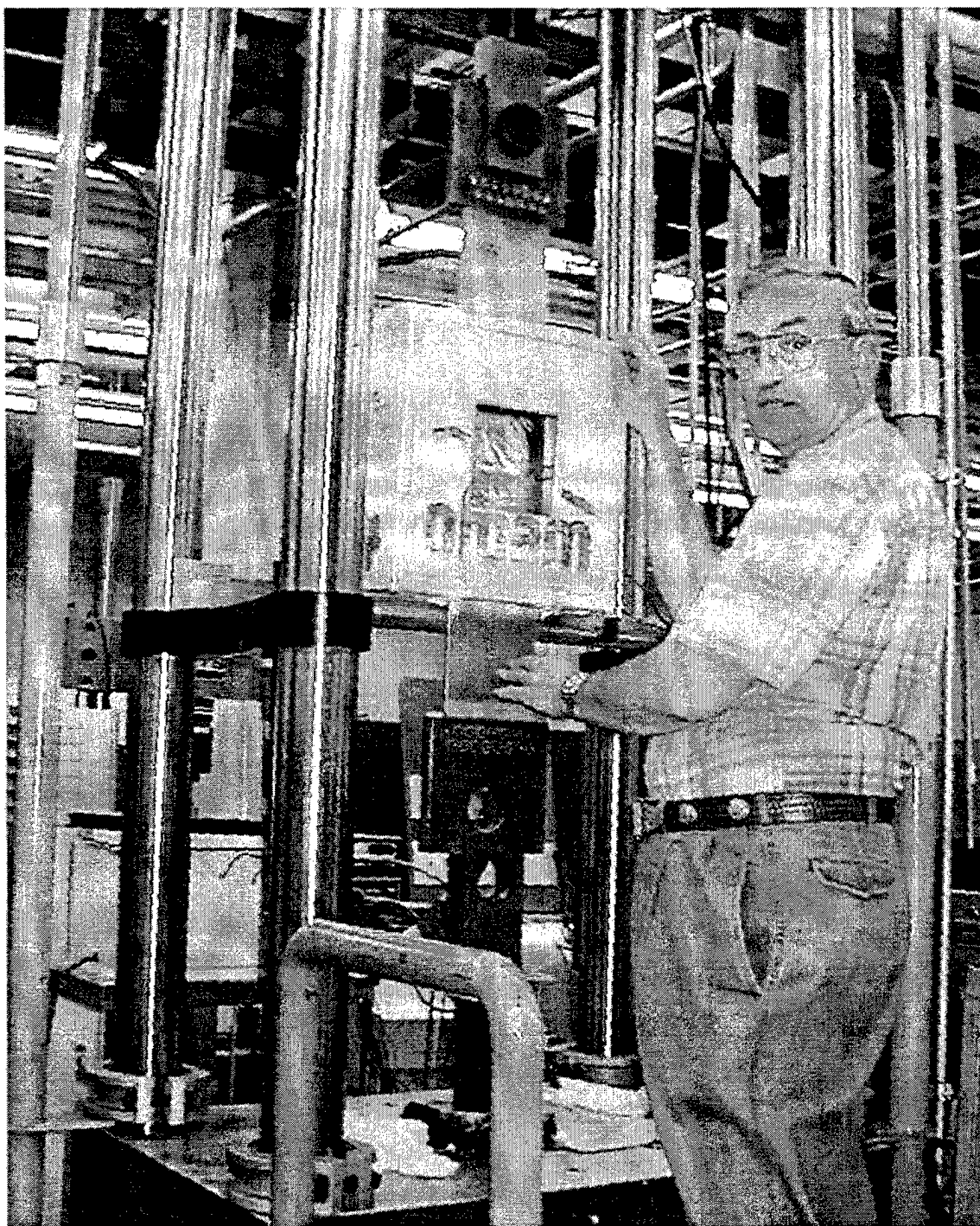
**Figure 8. Test Setup for 49 °C (120 °F) Tests**

21

4.6   FAILURE MODES

Each specimen was inspected after failure or termination of the test to identify failure mode. Most of the specimens failed either by a fracture somewhere within the aluminum substrate panel or were deemed to have failed because the extent of debonding between the patch and the aluminum substrate panel had reached such proportions as to render further fatigue cycling meaningless. A few specimens were terminated because no significant evidence of either metal or bond failure had occurred after extended fatigue cycling.

In a patched specimen, there are multiple possible failure locations. Failure modes that were observed during this investigation included those listed below, along with the abbreviation used to designate each. Figures 9 and 10 illustrate the failure mode described below:
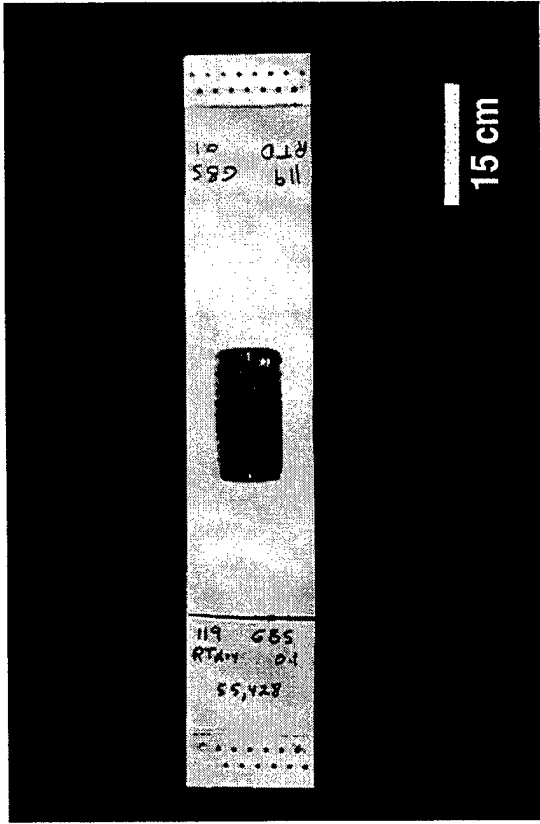
(a) Fracture of the aluminum substrate panel through the boltholes in the gripping area on the end of the specimen. This occurred on approximately 40% of the specimens. On nearly every one of these specimens interfacial debonding of the patch from the substrate aluminum panel also occurred and had been developing well before the bolthole fracture occurred. Where this type of failure occurred, and a more significant debonding mode of failure could not be attributed, it is designated as (G).

(b) Fracture of the aluminum substrate panel away from both the grip region and the patch region is designated as (M_a).

(c) Fracture of the aluminum substrate panel immediately adjacent to the end of the composite patch is designated as (M_e).

(d) Fracture of the aluminum substrate panel into two halves while the patch remains essentially intact on one or the other specimen halves. In this case the fracture of the metal under the patch is designated as (M_u). This failure mode also requires an identification of the failure locus where the patch pulled off the aluminum. In every case, it was one of the following three modes:

1. Cohesive failure within the adhesive layer is designated as (C).

2. Interfacial failure between the adhesive and the primer is designated as (I_{AP}).

3. Interfacial failure between the adhesive and the unprimed metal is designated as (I_{AM}).

The failure mode observed on each specimen was recorded after inspection. If multiple failure modes were present, the sequence in which they are listed indicates a progression from the most to the least prevalent mode observed. In some cases, particularly those in

Metal Fracture Away from Patch, M$_a$

Metal Fracture Under Patch, M$_u$
Cohesive Failure in Adhesive, C
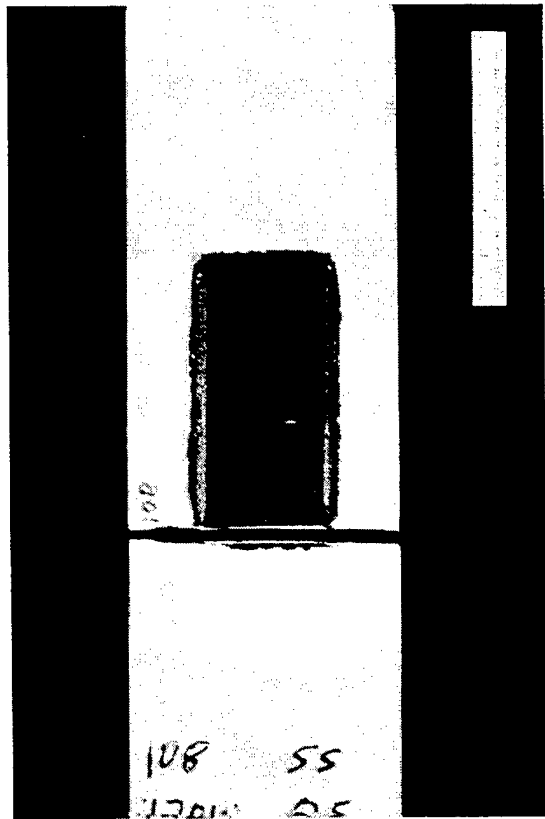
Metal Fracture at End of Patch, M$_e$

Figure 9. Noninterfacial Failure Modes Observed on Fatigue Specimens
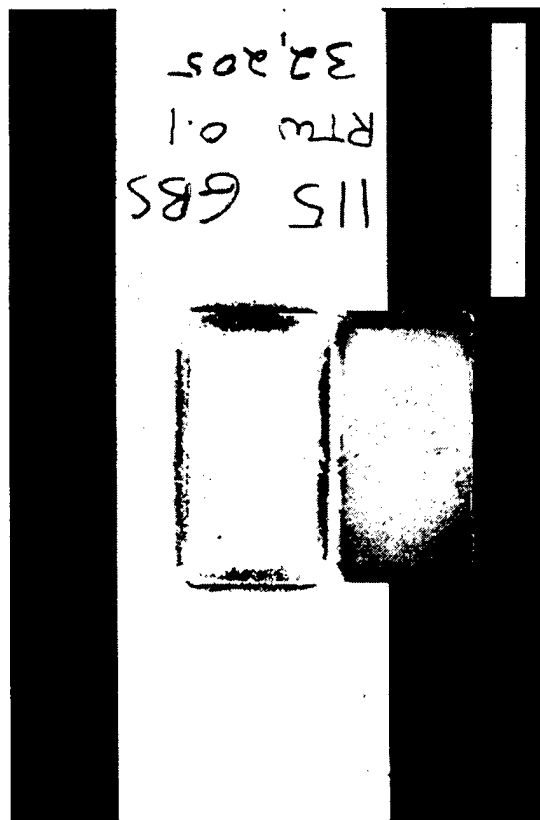
Interfacial Failure Between Primer and Adhesive, I_{ap}
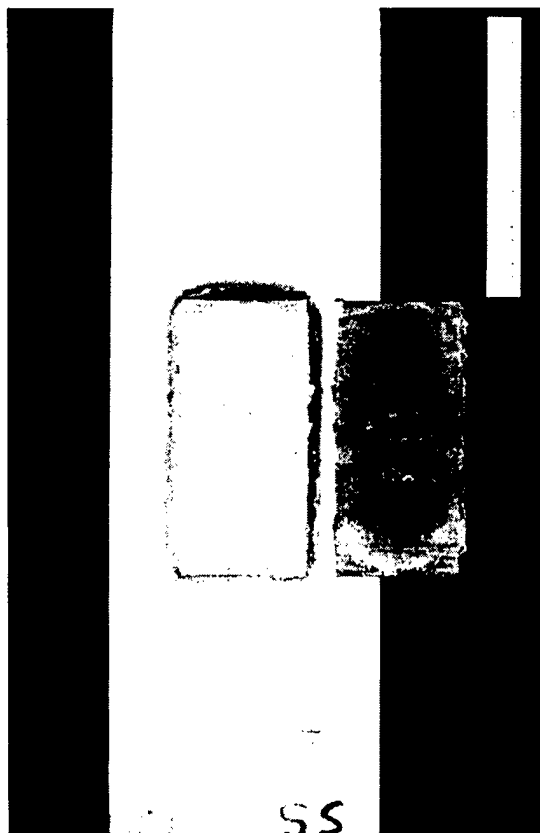
Interfacial Failure Between Metal and Adhesive, I_{ma}

Figure 10. Interfacial Failure Modes Observed in Fatigue Tests

which there was a grip (bolthole) failure, debonding was also observed between the patch and the substrate aluminum. If the extent of debonding was extensive, an effort was made to remove the patch from the aluminum so that the exact location of failure could be determined. In cases where this was done, the interfacial failure mode was listed as the predominant or only failure mode. A grip failure is indicated only for those cases where the patch could not be removed for direct determination of the interfacial failure location, or where the extent of debonding was not excessive.

The high incidence of grip failure in these tests is attributed to several factors. First, the high cyclic stress level (276 MPa; 40,000 psi) and the bolthole pattern in the specimen ends produced high stresses at the hole locations. Further, since the panels had no pre-cracks, the two points of stress concentration in the test panels were at the ends of the composite patch and the boltholes. If the patch disbonded from the panels, the only remaining stress concentration was the boltholes, so it is to be expected that failure would eventually be most likely to occur there. If the patch did not disbond from the panel, the eventual failure would be expected to occur at the sight of the highest stress concentration. The strain concentration around the boltholes is over 2 [Ref. 5] while that at the end of the patch is around 1.2-1.4 [Ref. 6]. Failure through the boltholes, therefore, is not surprising. The bolthole pattern used for these specimens has been successfully used for many previous fatigue tests without this grip failure problem. The difference appears to be in the higher stress levels encountered here and the environmental aging of the panels.

There is a correlation between the frequency of grip failure and the test condition. Only 1 of the 10 specimens tested at RTD and R=0.1 failed in the grips. That specimen failed at 28,000 cycles while those that did not fail in the grips survived for 11-56,000 cycles. For the RTD and R=0.5 test condition, neither of the two specimens failed in the grips and both ran for 140,000 or more cycles. For the RTW test condition at R=0.1, 4 of the 10 specimens failed in the grips at lifetimes of 16-32,000 cycles. Those that did not fail in the grips survived for 7-22,000 cycles. At RTW and R=0.5, neither of the two specimens failed in the grips, surviving for 32,000 and 90,000 cycles, respectively. For the 120W and R=0.1 test condition, both of the specimens tested failed in the grips at lifetimes of 10,000 cycles. For the 120W and R=0.5 test condition one of the two specimens failed in the grips of 66,000 cycles while the other failed at 63,000 cycles. In summary, the likelihood of grip failure in these tests increased with wet aging, with a lower cyclic stress ratio, and with a higher test temperature. This may be the result of the aging condition creating corrosion sites at the boltholes that acted as crack starters.

In retrospect, although a different bolthole design might have reduced the stress concentration, it may not have reduced it sufficiently to have eliminated the occurrence of failure at this location.

SECTION 5

DISCUSSION OF RESULTS

As would be surmised from the processing and test variables outlined in Tables 2 and 3, a substantial quantity of data was generated during this program. Sections 5.1 through 5.5 present and discuss the results of each of the tests and analyses performed during this effort. In these sections, the data presented in either tabular or graphical form represent average values if more than one replicate specimen was tested at any one condition.

Mechanical property data were generated for two different types of test specimens, as shown in Table 3. In the case of the wedge tests, the individual specimens were machined from a panel while in the case of the fatigue specimens, each specimen was a single panel. Wedge panels yielded five specimens each. A total of two wedge panels and 14 fatigue panels were made with each surface preparation. The two wedge panels were processed at the beginning and end of the fabrication of the fatigue panels with the composite patches.

5.1   STRAIN SURVEY TESTS

As described in Section 4.2, two specimens of each surface preparation were instrumented with five strain gages to measure panel strain at various locations during load application. All four of these specimens were tested in the room temperature dry condition. Load-strain measurements were obtained initially on all four instrumented specimens. One of the four specimens failed before a second set of strain readings could be obtained but for the other three specimens, additional sets of load-strain data were obtained after 10,000 and/or 20,000 load cycles. Figures 11 through 18 illustrate the results of these measurements.

In each of these figures, the strain behavior is similar. The gage mounted on the boron patch (1) exhibits compressive strains during initial load application. Since the panels are slightly curved as the result of the thermal expansion mismatch between the patch and the aluminum, gage 1 is on a convex surface. As load is applied to the panel, the curvature is straightened out, and the convex surface on which gage 1 is mounted experiences compression. Finally, when the tensile load is high enough to have fully straightened the panel (approximately 5000 lbs), gage 1 begins to exhibit tensile strain.

The initial behavior of gage 2 is the reverse of gage 1. Since it is mounted on the concave surface of the patched panel, the initial straightening load causes it to display an exaggerated tensile strain until the panel has been straightened out. After that, the rate of strain growth exhibited at this location is reduced relative to the far-field gages (4 and 5) because of the influence of the composite patch.

26

Panel 111
0 cycles

Gage 1
Gage 2
Gage 3
Gage 4
Gage 5

Load [lb.]
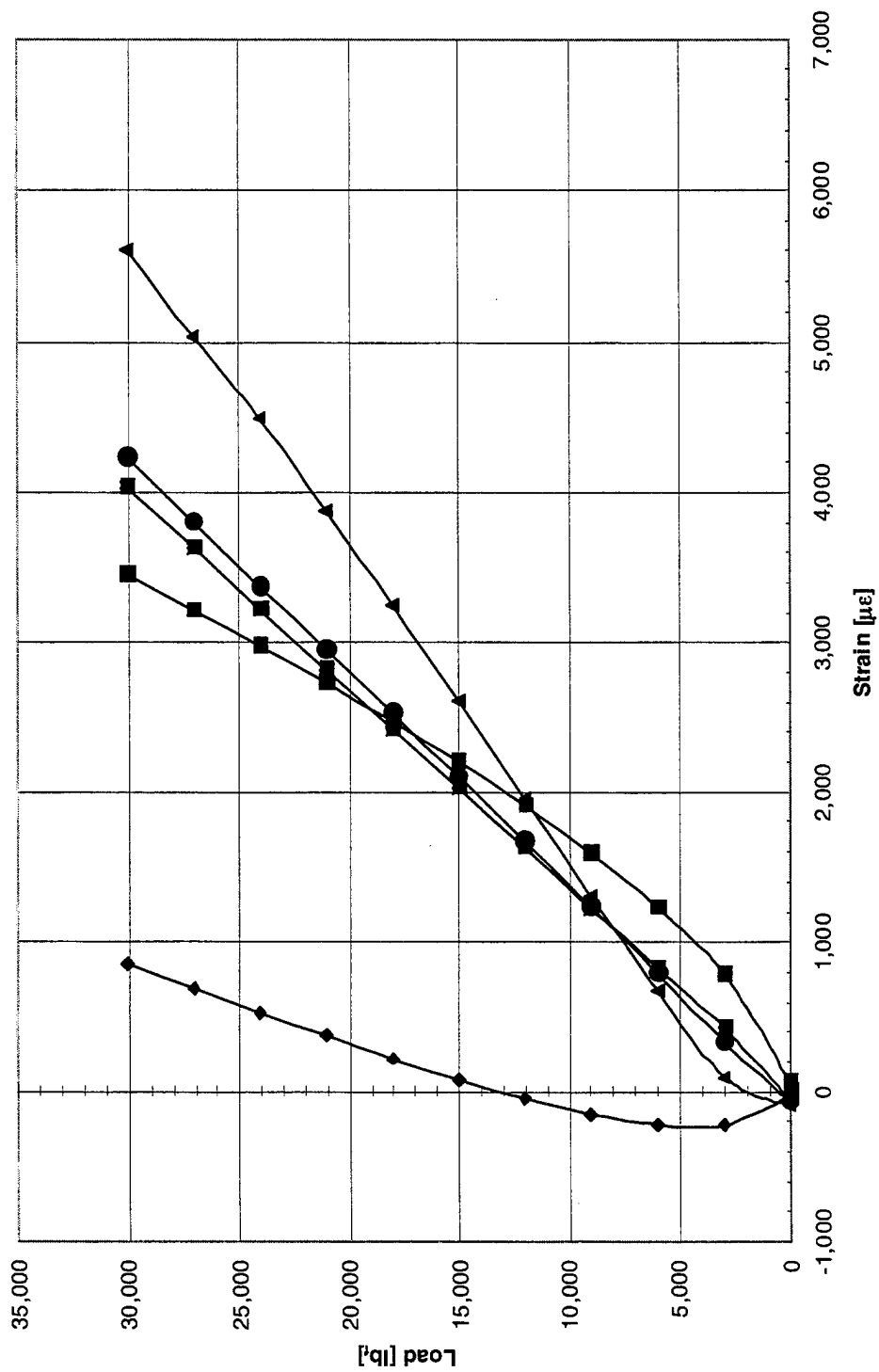
Strain [με]

Figure 11. Initial Load-Strain Survey for Panel 111; SS Surface Preparation
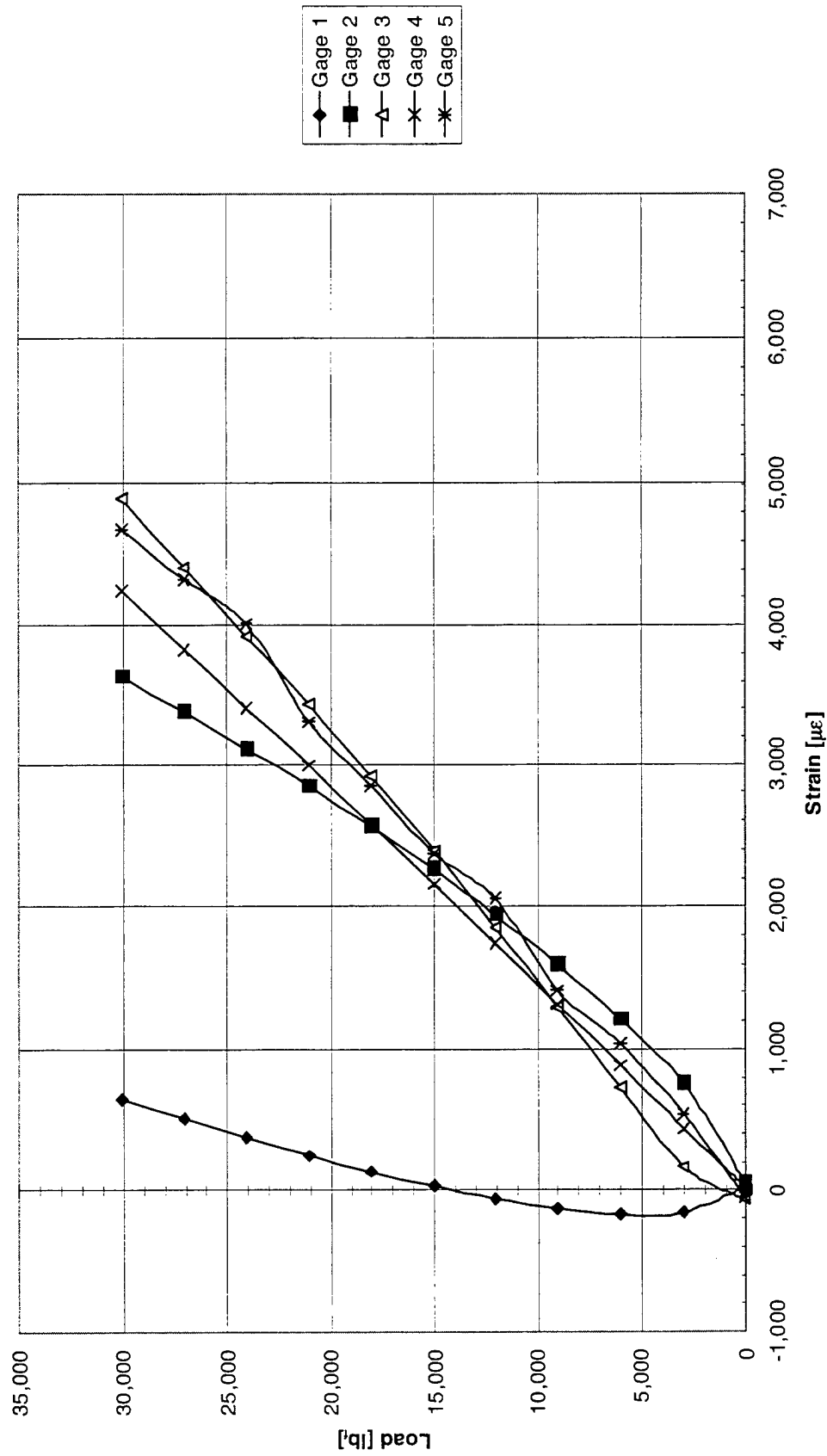
Figure 12. Load-Strain Survey for Panel 111 After 10,000 Cycles; SS Surface Preparation

28

Panel 111
20,000 cycles
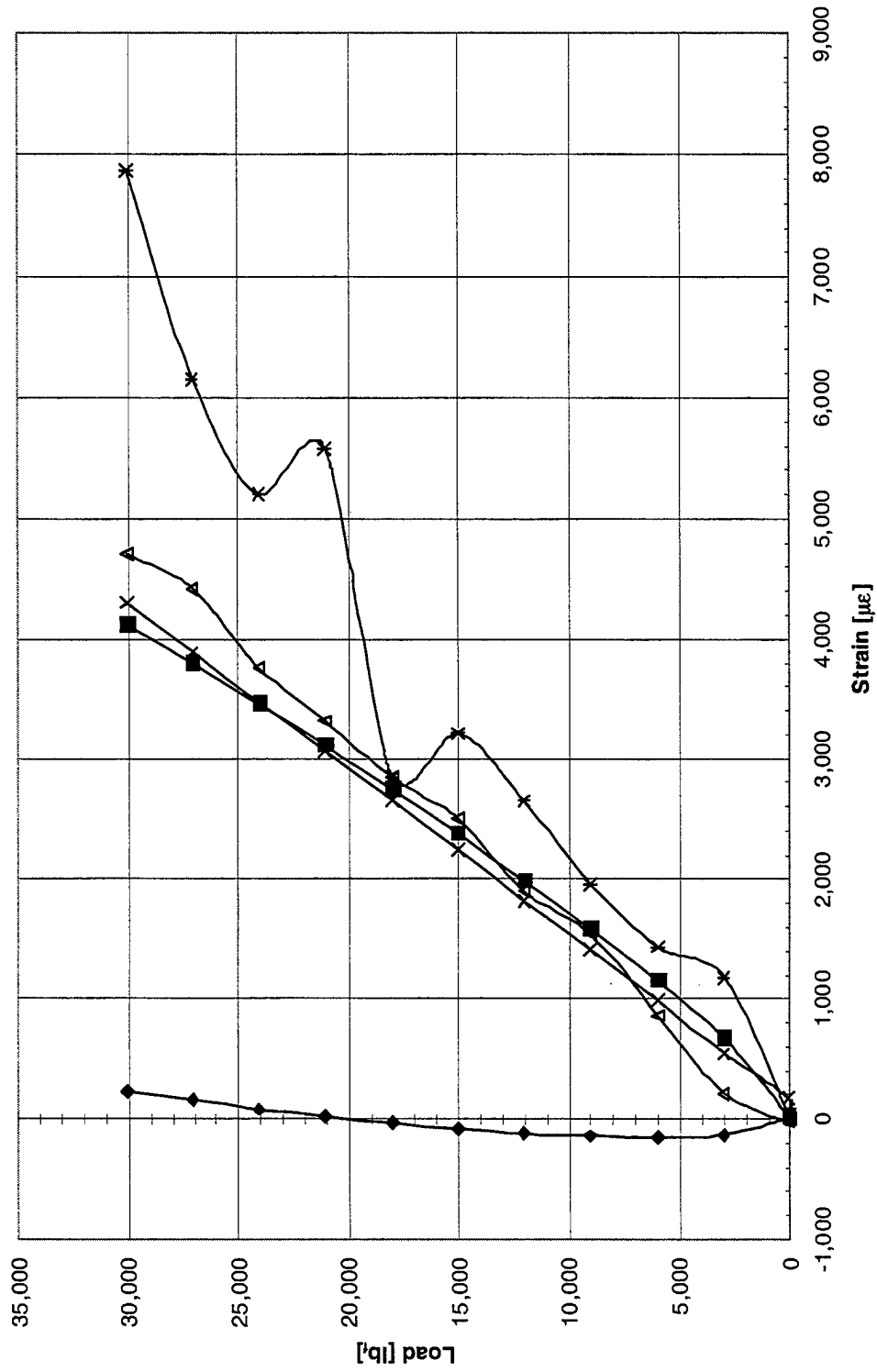
Figure 13. Load-Strain Survey for Panel 111 After 20,000 Cycles; SS Surface Preparation

29
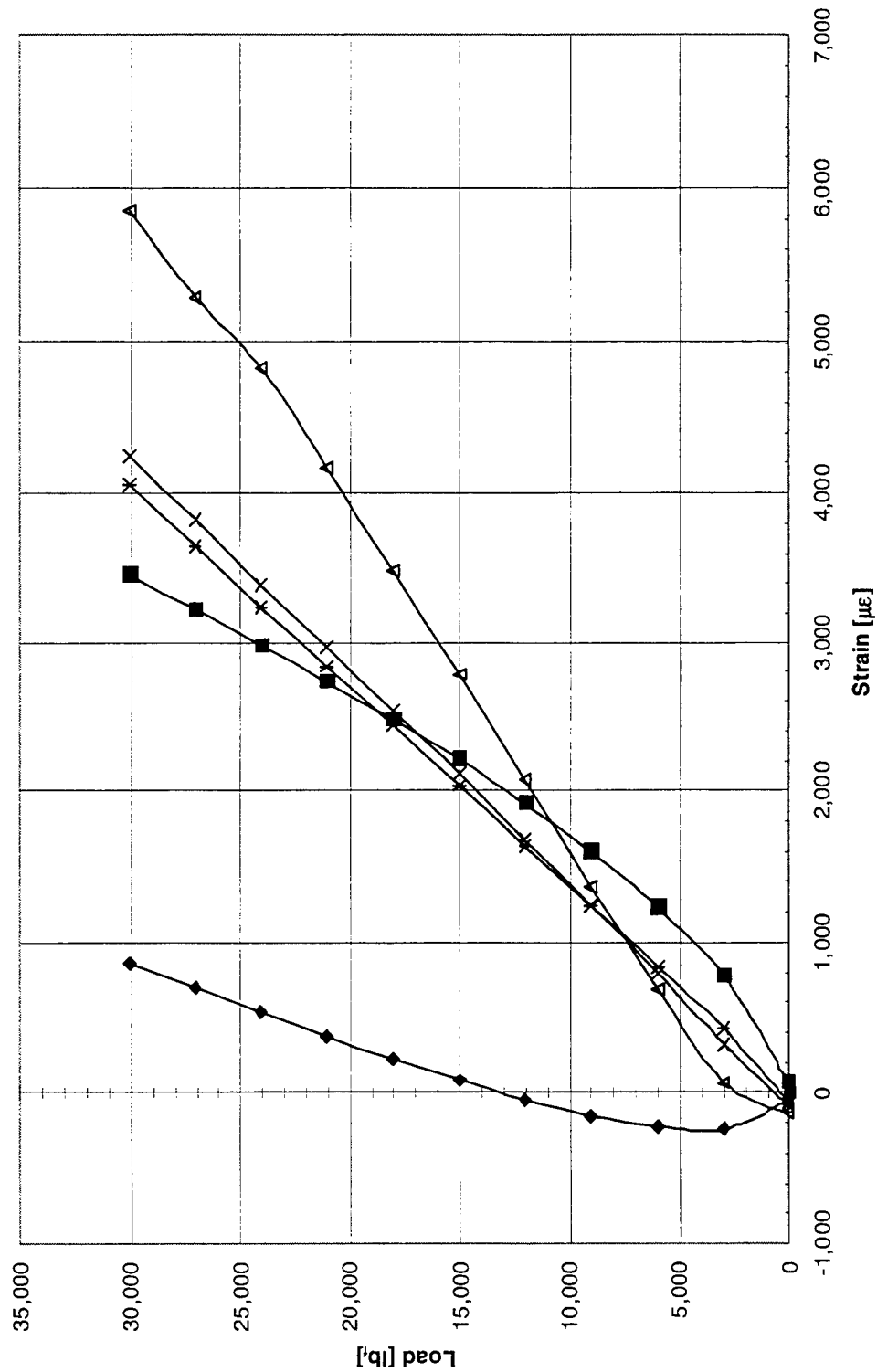
Panel 113
0 cycles

Figure 14. Initial Load-Strain Survey for Panel 113; SS Surface Preparation

30

Panel 113
10,000 cycles

Gage 1
Gage 2
Gage 3
Gage 4
Gage 5

Load [lb.]
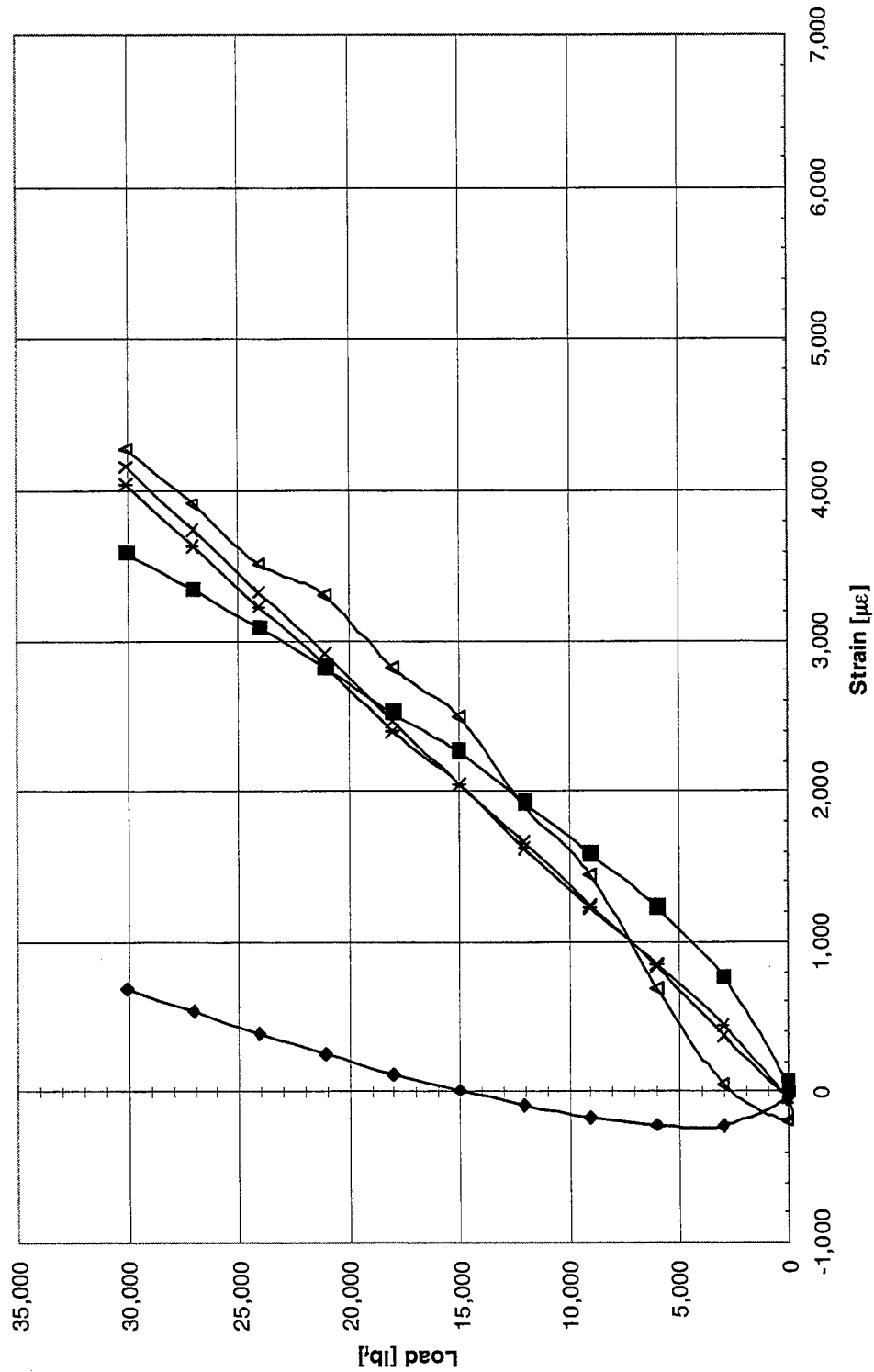
Strain [με]

Figure 15. Load-Strain Survey for Panel 113 After 10,000 Load Cycles; SS Surface Preparation

31

Panel 123
0 cycles

Figure 16. Initial Load-Strain Survey for Panel 123; GBS/BR127 Surface Preparation
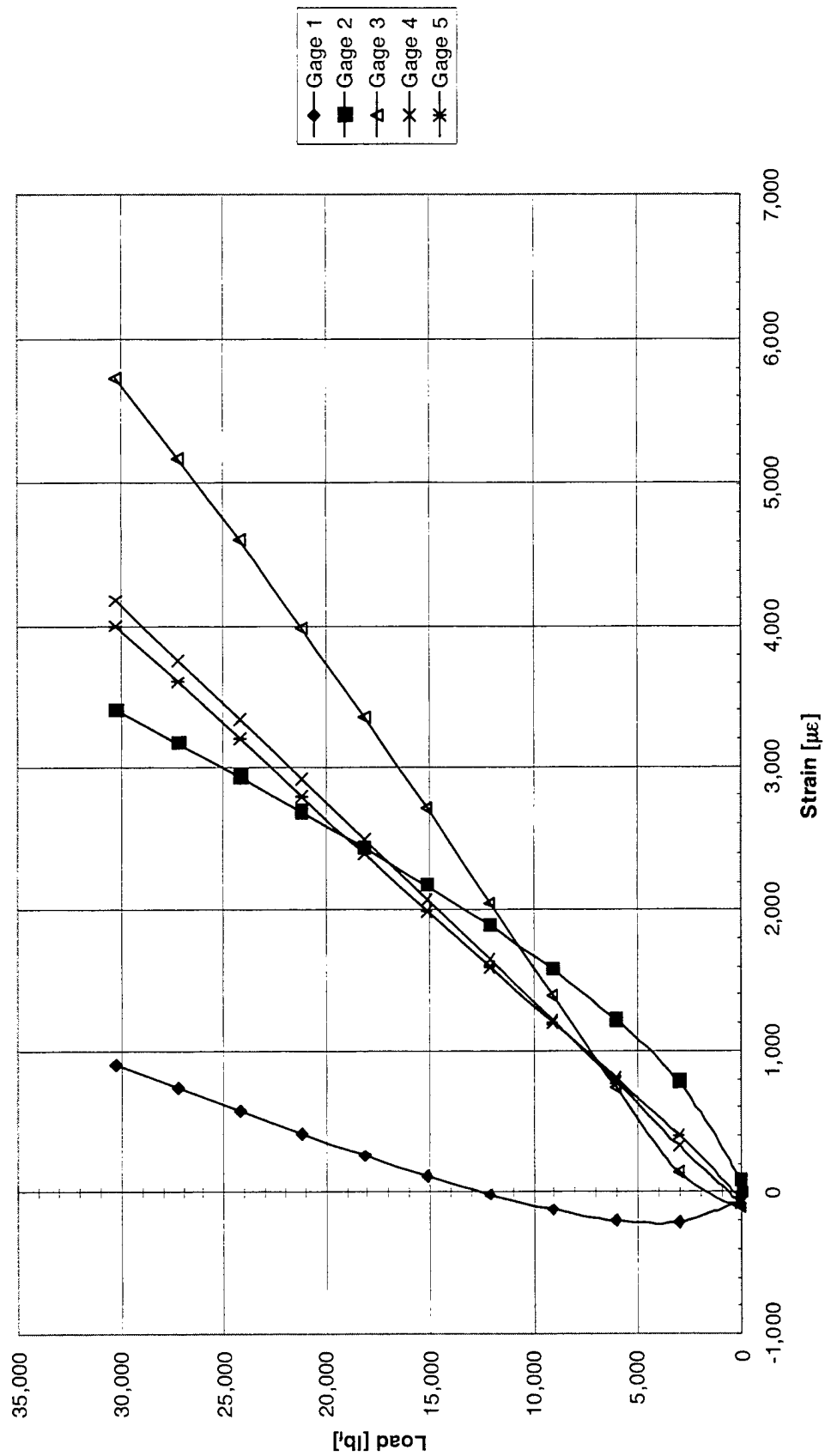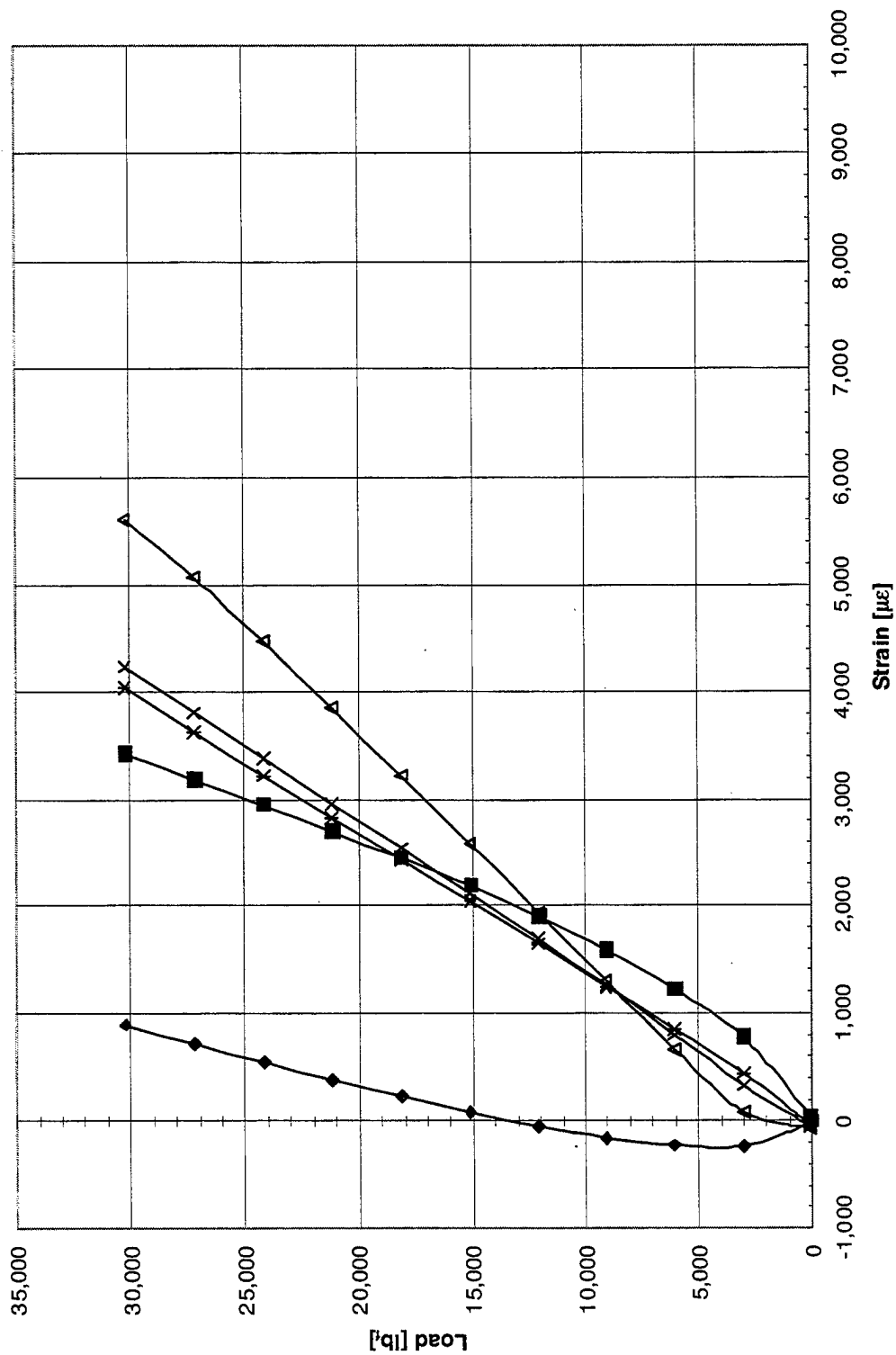
32

Panel 125
0 cycles

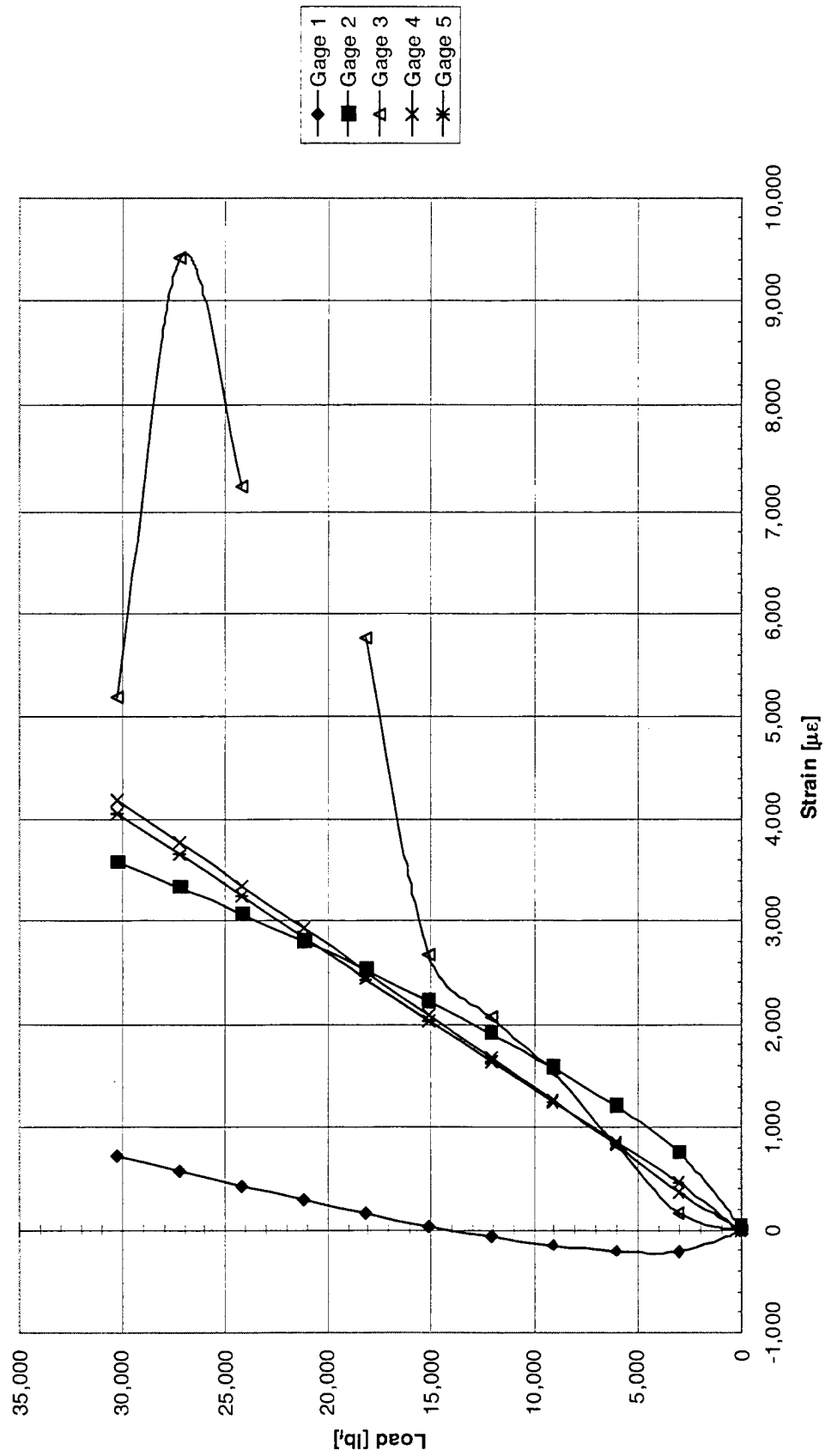Figure 17. Initial Load-Strain Survey for Panel 125; GBS/BR127 Surface Preparation

33

Figure 18. Load-Strain Survey for Panel 125 After 20,000 Load Cycles; GBS/BR127 Surface Preparation

34

Gage 3, which is located very close to the end of the boron patch, exhibits markedly higher strain than the two far-field gages. This is to be expected as a result of the stress concentration that exists at this location. An analysis provided by WR-ALC predicted a stress concentration factor of about 1.27 at the end of the patch used on these panels. At the start of load cycling, the ratio of the strain exhibited by the number 3 gages to that of the number 5 (far-field) gages on the four instrumented panels varied from 1.06-1.2 at 10,000 lb to around 1.4 at 30,000 lb tensile load.

After a number of load cycles had accumulated, the behavior exhibited by number 4 and number 5 gages remained close to that exhibited initially. The number 1 gages generally exhibit lower strains after cycling than initially. It is speculated that this is caused by a progressive debonding of the patch from the aluminum, thereby resulting in reduced load transfer into the patch. Concurrent with the reduced strains observed for the number 1 gages, the number 2 gages display higher strains after cycling than initially. This is also felt to be the result of the patch carrying reduced loads. The strain exhibited by the number 3 gages exhibit generally reduced strains as cycling progresses. This is attributed to the fact that the ends of the patches tend to become disbonded from the aluminum first. This effectively shifts gage number 3 further from the stress-concentration site at the end of the bond.

5.2 WEDGE CRACK-PROPAGATION TESTS

The wedge crack-propagation test has been acknowledged by most investigators to be an excellent, and perhaps the best, discriminator between environmentally durable and non-durable prebond surface treatments. One of the primary objectives in this program was to determine if a correlation existed between the wedge crack-propagation performance and the fatigue performance of the surface treatments. The results of the wedge crack-propagation tests are summarized in Table 4. Individual specimen wedge crack-propagation data are presented in Appendix C.

Table 4. Comparative Wedge Crack-Growth Behavior of Various Surface Preparations

Surface Prep	Cumulative Crack Length (in.)(1)							
	Exposure Time (hrs)							
	0	1	4	8	24	168	336	720
GBS/BR127	1.31	1.35	1.36	1.36	1.37	1.41	1.45	1.46
SS/ No Primer	1.21	1.46(A)	1.63(A)	1.73(A)	1.80(A)	1.86(A)	1.90(A)	1.98(A)

NOTE:
(1) Crack lengths shown represent averages of 10 specimens from two panels. Failure modes were 100 percent cohesive unless indicated otherwise by parenthetical notation of the number of specimens exhibiting adhesive failure.

35

It is immediately evident from these results that the GBS/BR127 surface preparation performed very well in the wedge tests, exhibiting low crack growth and cohesive failures throughout the tests. The SS/no-primer surface preparation, on the other hand, performed poorly, exhibiting high crack growth and an early onset of interfacial failure.

Based only on the wedge crack-propagation test results, the GBS/BR127 surface treatment appears to be far superior to the SS/no-primer surface preparation.

5.3 FATIGUE TESTS

The test specimens and procedures used for the fatigue tests were described in Section 4.5 and the fatigue test matrix was described in Section 2 and Table 3. In addition to the 28 fatigue specimens indicated by Table 3 (14 specimens/surface preparation times two surface preparations), 1 precracked aluminum specimen was tested.

As described in Sections 1, 2, and 5.2, one of the objectives of this program was to determine if a correlation exists between the wedge crack-propagation performance and fatigue performance for various prebond surface treatments. The results of the fatigue tests are presented in Tables 5 and 6. A number of different aspects of the fatigue data require discussion. These include the effects of stress ratio, test temperature, humidity pre-conditioning, and surface preparation. Each of these parameters is discussed in the following paragraphs.

Several features of the fatigue data in Tables 5 and 6 should be noted. First, for both surface preparations, the lifetime (number of cycles to failure) decreases as the test condition changes from RTD, to RTW, to 120W for a stress ratio (R) of 0.1. This is consistent with both the shifts in failure mode from condition-to-condition as well as the changes observed in the C-scan signature that will be discussed and illustrated in the following sections. In the case of the GBS/BR127 surface preparation, the failure mode changes from predominantly metal fracture away from, at the end of, or under the patch in the RT-dry condition, to interfacial between the primer and the adhesive in the two wet conditions. In the case of the SS/no-primer surface preparation, a significant amount of interfacial failure between the metal and the adhesive occurred for the RT-dry test condition and this same failure mode predominated at the RT-wet test condition.

A second feature of the fatigue data is the longer lifetime exhibited at a stress ratio of 0.5 relative to that at a stress ratio of 0.1. In the case of the GBS/BR127 specimens, the RT-wet specimen tested at R=0.5 survived nearly four times as many cycles as those tested at R=0.1. The 120°F-wet specimen with this surface preparation survived over six times as many cycles at R=0.5 as it did at R=0.1. In the case of the SS/no-primer specimens, the 120°F-wet specimen also survived over six times as many cycles at R=0.5 as it did at R=0.1. Only for the RT-wet condition on the SS/no-primer specimens was there no difference in lifetime between the two stress ratios. In this case they were about equal.

Lastly, comparison of the fatigue lifetimes for similar test conditions shows that the GBS/BR127 surface preparation exhibited equal or longer lifetimes than the SS/no-primer surface preparation.

36

Table 5. Fatigue Test Results for Specimens With GBS/BR127 Surface Preparation

Environmental Exposure (°F/%RH/days)	Test Condition (°F/%RH/R)(1)	Cycles to Failure	Failure Mode (2)
None	72/Dry/0.1	35,662	C, M_u
None	72/Dry/0.1	55,428	M_a
None	72/Dry/0.1	11,392	M_e
None	72/Dry/0.1	24,391	M_e
None	72/Dry/0.1	55,817	M_a
	Avg. ± Std. Dev.	36,538 ± 19,424	
None	72/Dry/0.5	>140,000	N.A.
160/100/225	72/Wet/0.1	32,205	I_{ap}, G
160/100/225	72/Wet/0.1	22,342	I_{ap}
160/100/247	72/Wet/0.1	17,539	I_{ap}
160/100/156	72/Wet/0.1	24,088	I_{ap}, G
160/100/273	72/Wet/0.1	19,634	I_{ap}
	Avg. ± Std. Dev.	23,162 ± 5,643	
160/100/249	72/Wet/0.5	90,000	I_{ap}
160/100/192	120/Wet/0.1	10,193	I_{ap}, G
160/100/208	120/Wet/0.5	66,385	I_{ap}, G

(1) WET indicates patched area of specimen was sealed inside a wet bag during testing to prevent dryout. R indicates fatigue stress-ratio (minimum/maximum).
(2) C = cohesive failure within adhesive
M_u = fracture of metal under patch
M_a = fracture of metal away from patch
M_e = fracture of metal at end of patch
G = fracture in grip area through boltholes
I_{ap} = interfacial failure between adhesive and primer

Table 6. Fatigue Test Results for Specimens
With SS/No-primer Surface Preparation

Environmental Exposure (°F/%RH/days)	Test Condition (°F/%RH/R)(1)	Cycles to Failure	Failure Mode (2)
None	72/Dry/0.1	47,326	I_{ma}, C, M_u
None	72/Dry/0.1	27,772	G, I_{ma}
None	72/Dry/0.1	46,141	I_{ma}, M_a
None	72/Dry/0.1	29,299	I_{ma}, M_a
None	72/Dry/0.1	13,209	M_e
	Avg. ± Std. Dev.	32,749 ± 14,233	
None	72/Dry/0.5	150,000	No failure, I_{ma} (3)
160/100/222	72/Wet/0.1	19,408	I_{ma}
160/100/154	72/Wet/0.1	16,087	I_{ma}, G
160/100/190	72/Wet/0.1	25,815	I_{ma}, G
160/100/249	72/Wet/0.1	6,738	I_{ma}, M_u
160/100/277	72/Wet/0.1	20,000	I_{ma}, M_u
	Avg. ± Std. Dev.	17,610 ± 7,014	
160/100/250	72/Wet/0.5	31,523	I_{ma}
160/100/208	120/Wet/0.1	10,519	G, I_{ma}
160/100/208	120/Wet/0.5	63,620	M_e, I_{ma}

(1) WET indicates patched area of specimen was sealed inside a wet bag during testing to prevent dryout. R indicates fatigue stress-ratio (minimum/maximum).

(2) C = cohesive failure within adhesive
M_u = fracture of metal under patch
M_a = fracture of metal away from patch
M_e = fracture of metal at end of patch
G = fracture in grip area through boltholes
I_{ma} = interfacial failure between metal and adhesive

(3) Specimen did not fail but C-scan and visual observation indicated some limited debonding of both ends of patch.

5.3.1 Effect of Surface Preparation on Retention of Bondline Integrity After Wet-Aging

The initial integrity of the bondline of each specimen was assessed by means of a nondestructive C-scan inspection, as described in Section 4.5. The wet-aged specimens were inspected after the wet-aging period had been completed but before any load cycles had been applied. Comparison of the initial C-scans of the dry unaged and wet-aged specimens reveals no differences in the initial bondline integrity of the two different surface preparations. For both the GBS/BR127 and SS/no-primer surface preparations, the duration of the 160°F, 100%RH aging did not exhibit any consistent effect on C-scan appearance. Figure 19 illustrates typical C-scans for both unaged specimens and aged specimens that had been in wet-aging for 9 months.

Although there was no apparent deleterious effect on the bondline integrity as determined by a C-scan, this does not mean that the bonds on the two different surface preparations were of equivalent strength. It only indicates that the path for transmission of an ultrasonic signal through the bondline was equally continuous for both surface preparations at the conclusion of wet-aging but before load application.

5.3.2 Effect of Surface Preparation on Retention of Bondline Integrity During Fatigue

As described in Section 4.5, the periodic C-scans tracked bondline integrity during the fatigue testing. In addition to the C-scans, operator observations were recorded as fatigue cycling progressed. These included the appearance of observable cracks around the periphery of the patches, relative movement of the end of a patch with respect to the underlying aluminum substrate, and whether the end of a patch lifted off the aluminum if the panel were slightly bowed.

In order to quantify changes in the appearance of the C-scans as load cycles accumulated, the percent of the patch area that exhibited a signal attenuation of 50 percent or less, relative to the lowest attenuation level for a well-bonded patch, was measured and recorded at each inspection interval. Figures 20 through 23 illustrate the C-scans for several typical specimens as fatigue load cycles accumulated and illustrate the progressive degradation of the bondline. As described in Section 4.1, it must be kept in mind that although these figures are presented in black/white/shades-of-gray, the original C-scans were in color. The signal attenuation levels at various locations in the bondlines are much more readily discerned on the colored originals than on the black/white/shades-of-gray copies incorporated into this report. For the C-scans in Figures 20 through 23, the portion of each bondline that remains undegraded is outlined by a black tracing and labeled G, where the G signifies this area is still as good as it appeared on the initial C-scan before load cycling started.

Specimen No. 117	Specimen No. 124	Specimen No. 103	Specimen No. 101
GBS/BR127 Surface Preparation	GBS/BR12.7 Surface Preparation	SS/No Primer Surface Preparation	SS/No Primer Surface Preparation
No Aging	247 Days Aging @ 160°F, 100% RH	No Aging	222 Days Aging @ 160°F, 100% RH
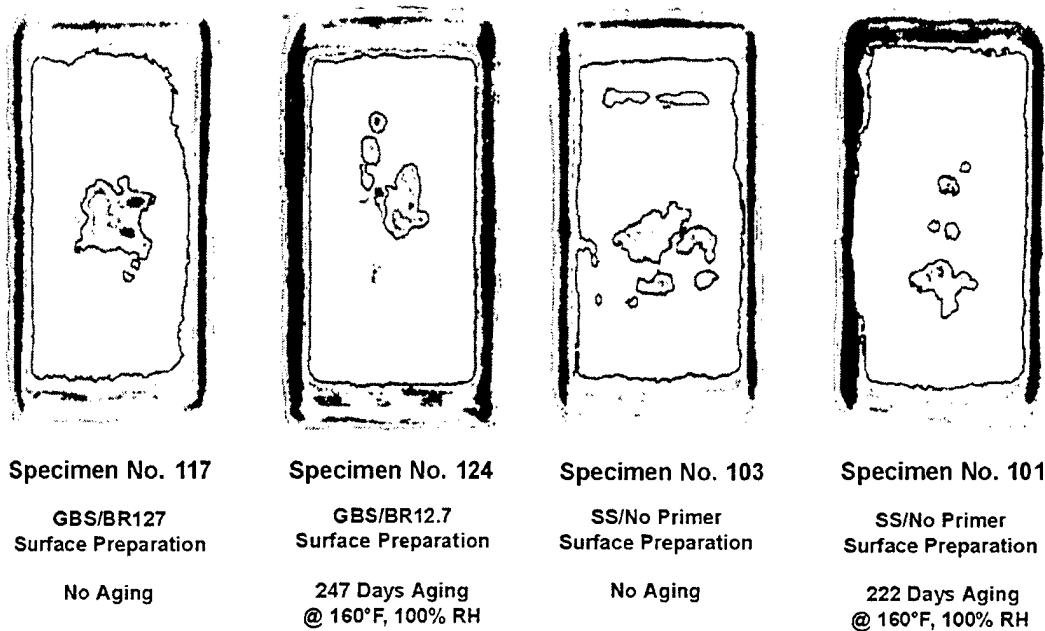
Figure 19. Effect of Wet-Aging on Bondline Integrity as Indicated by C-Scans

For each specimen, the ratio of the remaining good or undegraded portion of the bondline to the original good portion of the bondline was determined at each C-scan inspection. This ratio represents a quantified measure of bondline integrity. Figures 24 through 28 illustrate how this bondline integrity, measured as described above, changes with fatigue cycling for various test conditions. In these figures, the lines plotted for the room temperature-dry and room temperature-wet test conditions at R=0.1 represent least-square fits of the data for five specimens each. The values for r given for each line represents the least-squares correlation coefficient. The lines for the other test conditions represent a single specimen each.

Inspection of the curves in Figures 24 through 28 along with the failure modes tabulated in Tables 5 and 6 leads to the observations described in the following subsections.

0 CYCLES
100% Bondline Integrity

20,000 CYCLES
98% Bondline Integrity

40,000 CYCLES
93% Bondline Integrity

55,817 CYCLES
88% Bondline Integrity
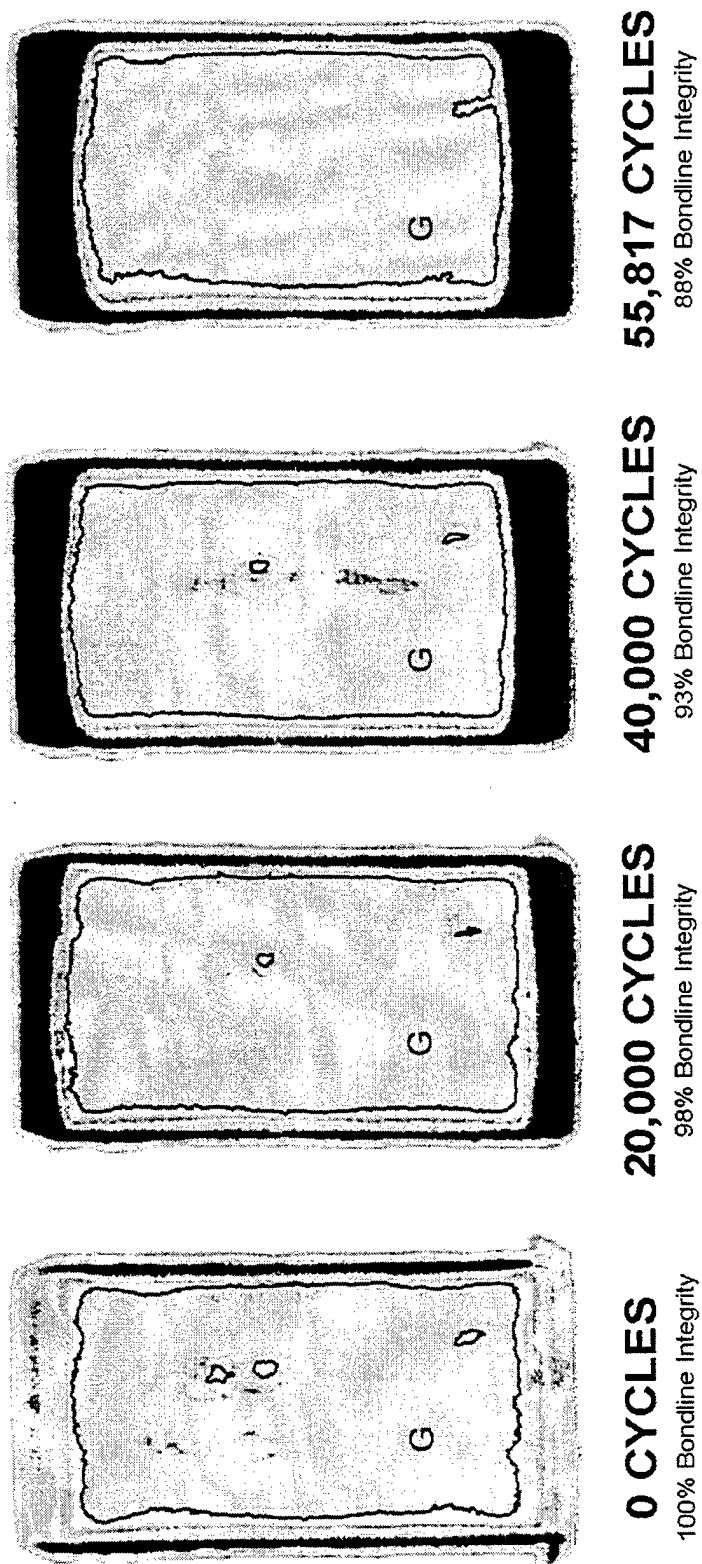
Specimen No.: 127
Surface Preparation: Grit-Blast Silane/BR127
Test Condition: Room Temperature Dry
Fatigue Stress Ratio: 0.1

Figure 20. Effect of Fatigue Cycling on Bondline Integrity as Indicated by C-Scans

0 CYCLES
100% Bondline Integrity

5000 CYCLES
75% Bondline Integrity

20,000 CYCLES
75% Bondline Integrity

24,088 CYCLES
20% Bondline Integrity
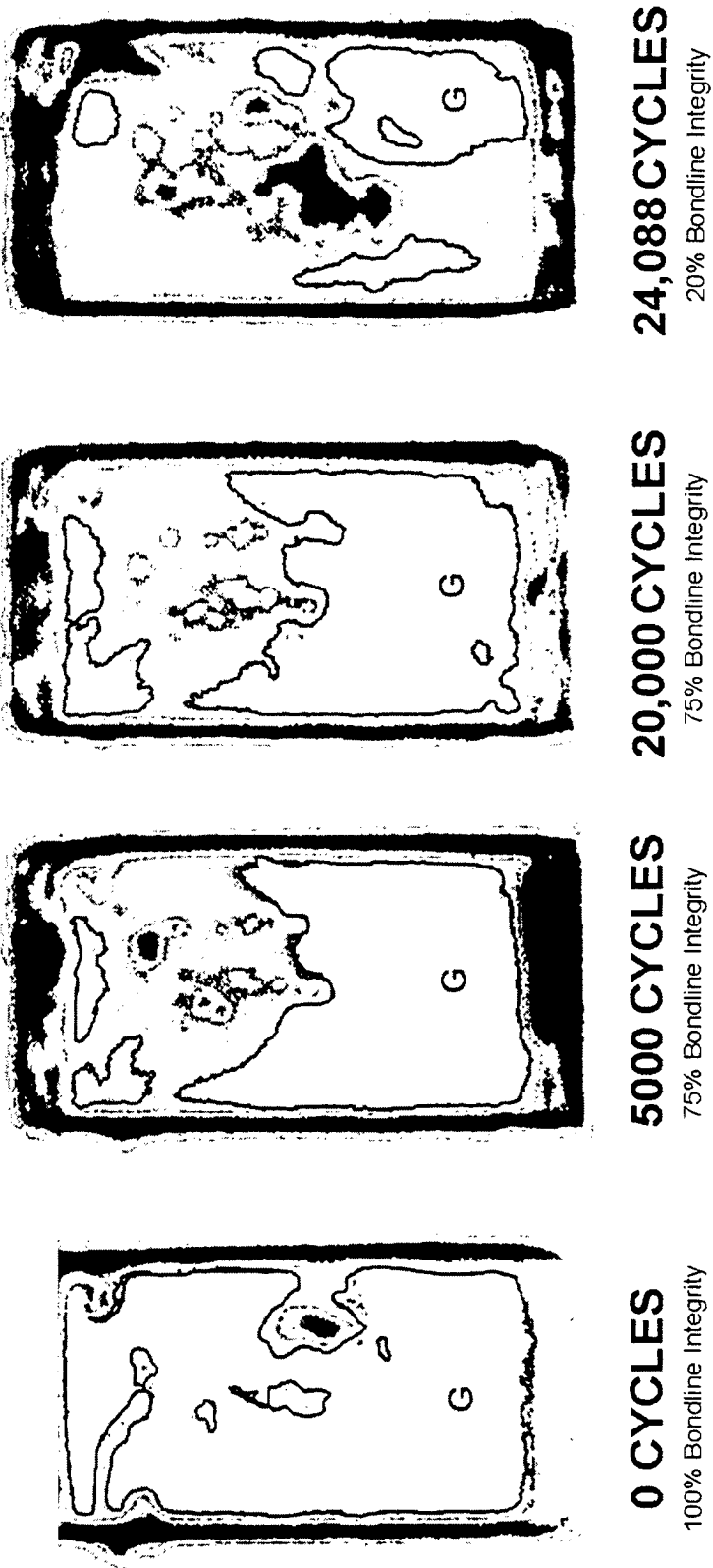
Specimen No.: 126
Surface Preparation: Grit-Blast Silane/BR127
Test Condition: Room Temperature Wet
Fatigue Stress Ratio: 0.1

Figure 21. Effect of Fatigue Cycling on Bondline Integrity as Indicated by C-Scans

42

0 CYCLES
100% Bondline Integrity

10,000 CYCLES
98% Bondline Integrity

20,000 CYCLES
70% Bondline Integrity

41,800 CYCLES
30% Bondline Integrity
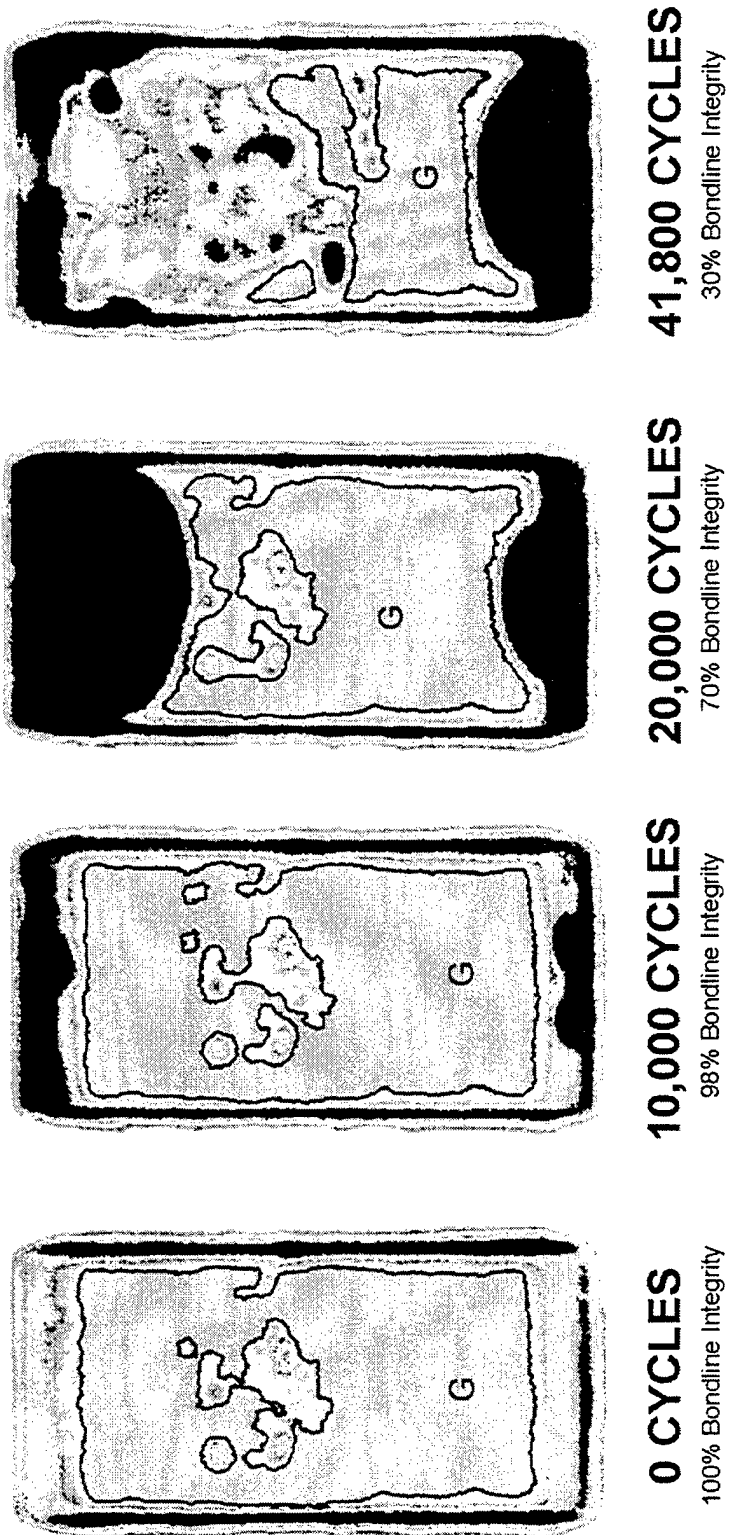
Specimen No.: 103
Surface Preparation: Scuff-Sand/No Primer
Test Condition: Room Temperature Dry
Fatigue Stress Ratio: 0.1

Figure 22. Effect of Fatigue Cycling on Bondline Integrity as Indicated by C-Scans

43

0 CYCLES

100% Bondline Integrity

10,000 CYCLES

50% Bondline Integrity

15,000 CYCLES

29% Bondline Integrity

19,408 CYCLES

14% Bondline Integrity
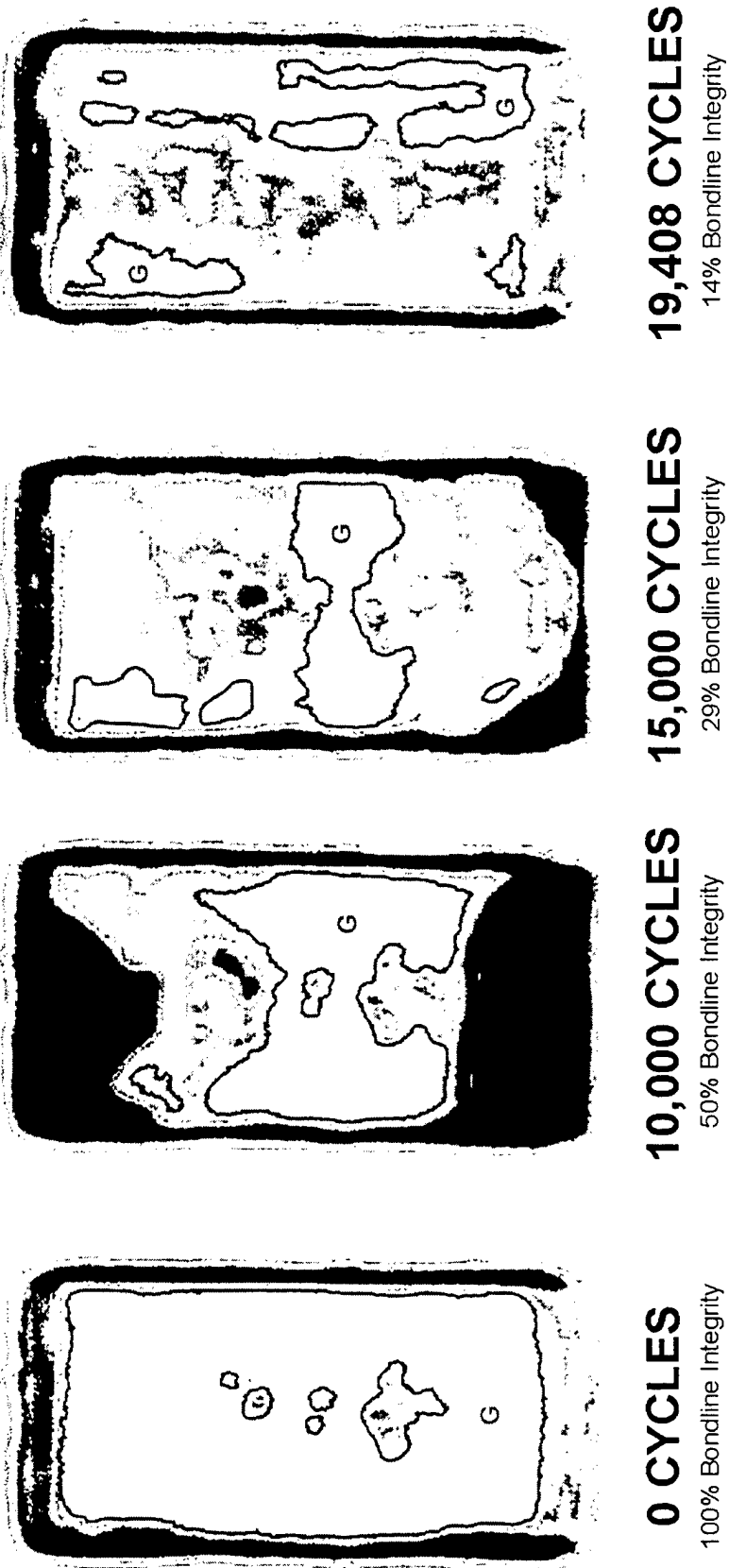
Specimen No.: 101
Surface Preparation: Scuff-Sand/No Primer
Test Condition: Room Temperature Wet
Fatigue Stress Ratio: 0.1

Figure 23. Effect of Fatigue Cycling on Bondline Integrity as Indicated by C-Scans

44

Figure 24. Effect of Fatigue Cycling on Bondline Integrity of Patched Specimens Tested at Room Temperature and at a Stress Ratio of 0.1

45

Figure 25. Effect of Fatigue Cycling on Bondline Integrity of Patched Specimens Tested in the Wet Condition and at a Stress Ratio of 0.1

Figure 26. Effect of Fatigue Cycling on Bondline Integrity of Patched Specimens Tested at a Stress Ratio of 0.5

47

Figure 27. Effect of Fatigue Cycling on Bondline Integrity of Patched Specimens With a GBS/BR127 Surface Preparation
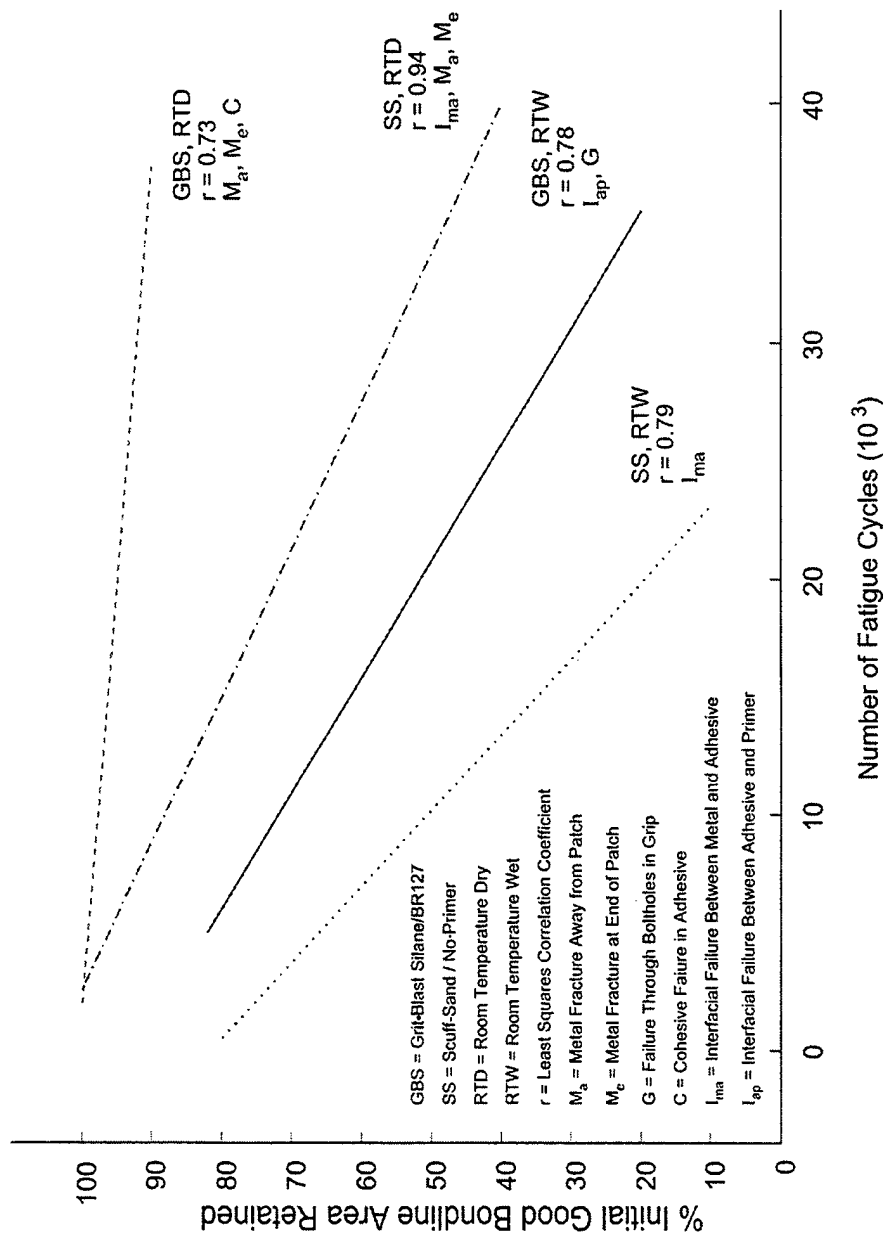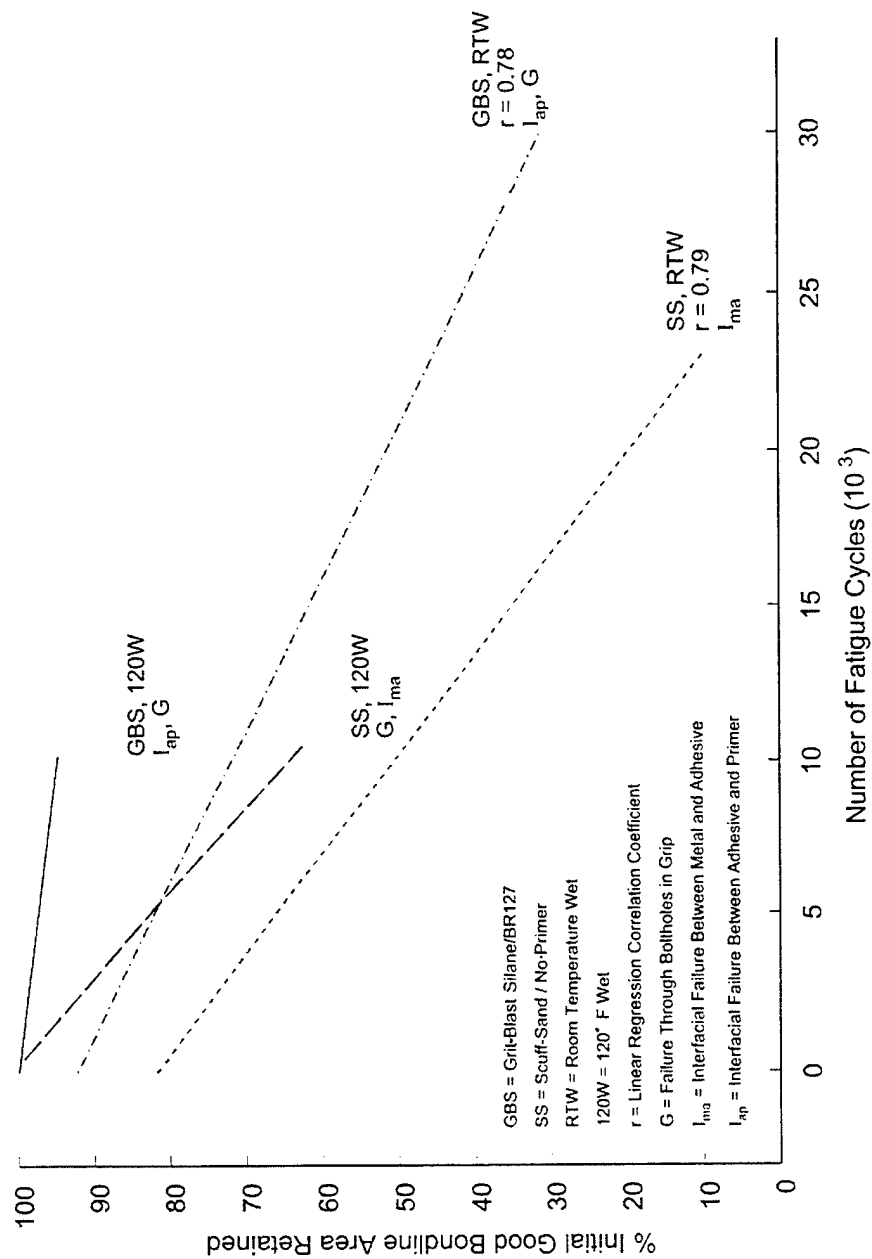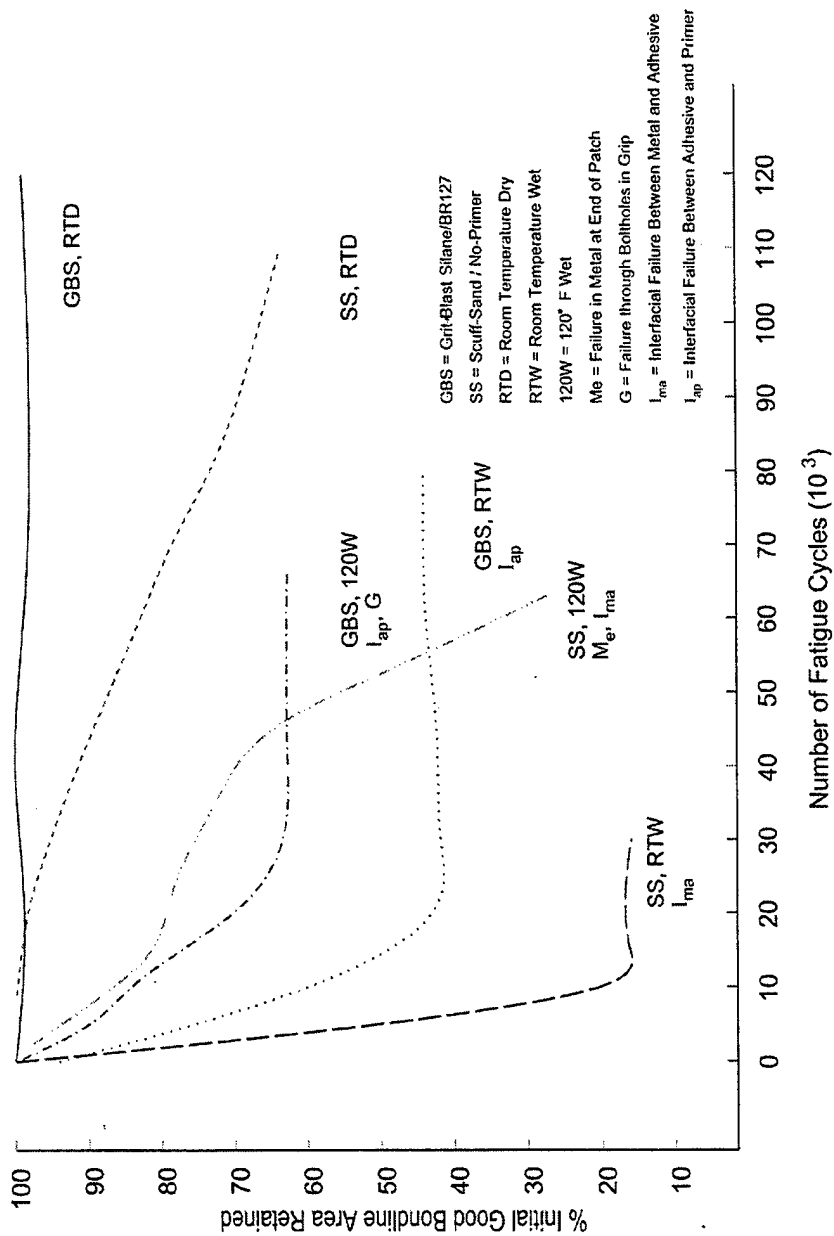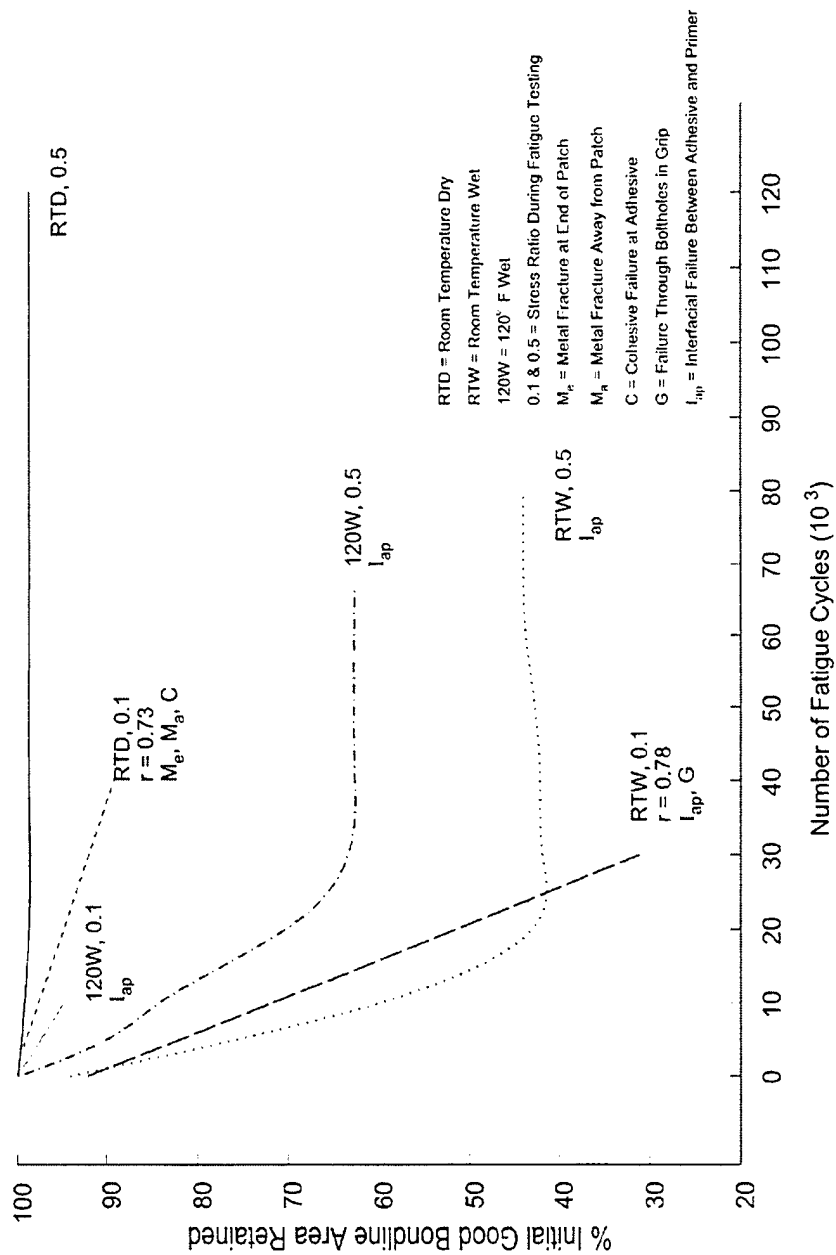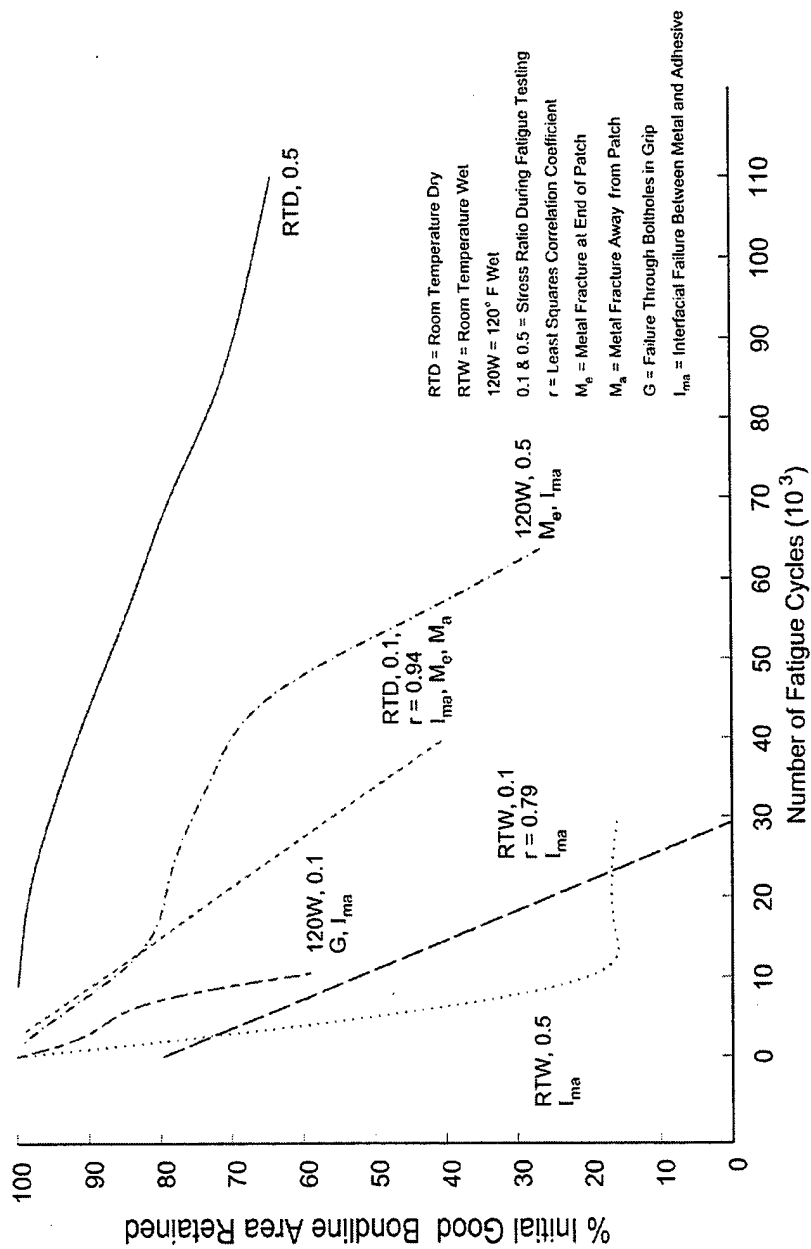
Figure 28. Effect of Fatigue Cycling on Bondline Integrity of Patched Specimens With a Scuff-Sand/No-Primer Surface Preparation

5.3.2.1 *Effect of Surface Preparation on Fatigue Performance*

There are six combinations of test conditions for which the two different surface preparations used in this investigation can be compared. These include two test temperatures (room temperature and 120 °F), two aging conditions (dry and wet), and two cyclic stress ratios (0.1 and 0.5). Figures 24 through 28 illustrate the comparative resistance of these two surface preparations to degradation during fatigue cycling. Each of these figures plots the bondline integrity (ratio of remaining good bond area to original good bond area, as determined from C-scans) versus the number of fatigue cycles. The following paragraphs each focus on a single combination of test parameters and compare the behavior of the GBS/BR127 surface preparation to the SS/no-primer surface preparation. It will become apparent that the GBS/BR127 surface preparation proves to be consistently superior, as would be expected.

Room Temperature Dry Tests at R=0.1

Figure 24 shows that while the bondlines of the GBS/BR127 specimens exhibited 10 percent loss of overall integrity after 40,000 fatigue cycles, the SS specimens lost 60 percent of their overall integrity after 40,000 fatigue cycles. This disparity is supported by a difference in failure mode. The GBS/BR127 specimens failed predominantly in the metal outside the patch area with the patches remaining firmly bonded to the aluminum. Four of the five SS specimens also exhibited failure in the metal but it was accompanied by visible disbonding of the patches on at least one end. Removal of these patches revealed that the loss of bond integrity evident in the C-scans was due to interfacial failure between the adhesive and the aluminum. For this test condition, the GBS/BR127 surface preparation is clearly more durable than the SS surface preparation.

Room Temperature Wet Tests at R=0.1

It can be seen in Figure 24 that although the GBS/BR127 and SS surface preparations lose considerable bondline integrity during fatigue cycling of wet-aged specimens at room temperature, the SS specimens degrade more rapidly than the GBS/BR127 specimens. The GBS/BR127 specimens lose about 70 percent of their initial bond integrity after 30,000 fatigue cycles while the SS specimens lose approximately 80 percent of their initial bond integrity after only 20,000 fatigue cycles. The loss of bond integrity on the GBS/BR127 specimens occurs along the adhesive-primer interface (I_{ap}) while the degradation on the SS specimens is along the adhesive-metal interface (I_{ma}). For this test condition, the GBS/BR127 surface preparation is clearly more durable than the SS surface preparation. The greater durability of the GBS/BR127 specimens is presumably attributable to both the greater environmental durability of the GBS surface treatment and the corrosion inhibiting BR127 primer.

50

<u>120 °F Wet Tests at R=0.1</u>

Figure 25 shows that the GBS/BR127 surface preparation loses about 5 percent of its bond integrity after 10,000 fatigue cycles while the SS surface treatment loses about 35 percent. In both cases, the specimens failed through the boltholes in the grip between 10,000 and 11,000 cycles. The patches on both surface preparations showed slight debonding on each end but they were still bonded firmly enough that they could not be removed for direct inspection of the interface. Based on the relative loss of bond integrity, the GBS/BR127 is clearly a more durable surface preparation than the SS.

<u>All Three Test Conditions at R=0.5</u>

Figure 26 illustrates the change in bondline integrity for both surface preparations at all three test conditions for a fatigue stress-ratio of 0.5. It is evident from the curves in this figure that for each of the three test conditions (RTD, RTW, and 120W) the GBS/BR127 surface preparation does not deteriorate as much as the SS surface preparation.

For the RTD condition, the GBS specimen retains practically all of its original bondline integrity after 140,000 cycles while the SS specimen retains about 65 percent of its original bondline integrity after 110,000 cycles. Neither specimen failed so the fatigue test was terminated after 140,000 cycles for the GBS/BR127 specimen and 150,000 cycles for the SS specimen. As a result, a direct observation of failure modes was not obtained.

For the RTW condition, the GBS/BR127 surface preparation rapidly lost 50-60 percent of its initial bondline integrity, then exhibited no further change. The SS surface preparation, on the other hand, rapidly lost 80 percent of its initial bondline integrity then leveled off. The predominant failure in both cases was interfacial with the GBS/BR127 failure occurring along the adhesive-primer interface (I_{ap}) while the SS failure was along the adhesive-metal interface (I_{ma}).

For the 120W condition, both specimens failed at around 65,000 fatigue cycles. The GBS/BR127 specimen failed through the boltholes in the grip area while the SS specimen failed through the metal right at the end of the patch. Both specimens exhibited interfacial failure at the ends of the patch, the GBS/BR127 specimen at the adhesive-primer interface (I_{ap}), and the SS specimen at the adhesive-metal interface (I_{ma}).

For each of the three test conditions at a cyclic stress-ratio of 0.5, the GBS/BR127 surface preparation exhibited greater retention of bondline integrity than the SS surface preparation.

In summary, for each of the comparisons discussed above, the GBS/BR127 surface preparation proved more resistant to environmental and fatigue degradation than the SS

51

surface preparation. Table 7 summarizes the comparative failure modes for the two different surface preparations at the various test conditions.

Table 7. Patched Fatigue Specimen Failure Modes

Surface Preparation	Fatigue Stress Ratio	Test Condition		
		RT Dry	RT Wet	120 °F Wet
GBS/BR127	0.1	M_a	I_{ap}	I_{ap} (1)
SS/No primer	0.1	I_{ap}	I_{ma}	I_{ma} (1)
GBS/BR127	0.5	NA (2)	I_{ap}	I_{ap}
SS/No primer	0.5	NA (3)	I_{ma}	I_{ma}

M_a = Failure in metal away from patch.

I_{ap}= Interfacial failure between metal and adhesive.

I_{ma}= Interfacial failure between metal and adhesive.

NA= Failure mode not available because no failure occurred.

(1) These failure modes were observed only under the slightly debonded ends of the patch. The tests were prematurely terminated by grip failure through the boltholes.

(2) Test was terminated at 140,000 cycles with no failure and no evidence of patch disbonding.

(3) Test was terminated at 150,000 cycles with no failure. C-scan indicated limited disbonding of both ends of patch.

5.3.2.2 Effect of Wet-Aging on Fatigue Performance

The effects of wet-aging the patched specimens prior to fatigue testing can be compared by comparing the bondline integrity curves for the GBS/BR127 and SS/no-primer surface preparations at both R=0.1 and R=0.5 in Figures 24 and 26.

First, in Figure 24, the RTD and RTW conditions can be compared for both surface preparations at R=0.1. It is obvious that the degradation of bondline integrity occurs much more rapidly for the RTW test condition than for the RTD condition. In the case of the GBS/BR127 surface preparation, the failure mode changes from predominantly metal failure in the RTD condition, near to or far from the patch (M_e or M_a), to predominantly interfacial failure between the adhesive and the primer (I_{ap}) in the RTW condition. In the case of the SS/no-primer surface preparation, both test conditions produced significant interfacial failure between the adhesive and the metal (I_{ma}) but the RTD condition also produced some metal failure.

The curves plotted in Figure 26 permit comparison of the RTD and RTW conditions for R=0.5. For both the GBS and SS surface preparations the RTW test condition causes much more rapid and severe degradation of the bondline integrity than the RTD condition. For the RTD condition both surface preparations survived 140-150,000 fatigue cycles with the patch still firmly bonded to the aluminum panel, even though in the case of the SS/no-primer specimen, there was evidence that both ends of the patch had

started to disbond from the panel. For the RTW condition the bondline integrity deteriorated very rapidly and very significantly during the first 10-20,000 fatigue cycles with the GBS/BR127 specimen failing along the adhesive-primer interface (I_{ap}) and the SS/no-primer specimen along the adhesive-metal interface (I_{ma}).

In summary, as would be expected the wet-aged specimens tested in the RTW condition were much less durable than the unaged specimens tested in the RTD condition.

5.3.2.3 *Effect of Test Temperature on Fatigue Performance*

The effect of test temperature can be observed by comparing the behavior of specimens tested at the RTW condition to that of specimens tested at the 120W condition, all other things being equal. Figures 25 and 26 illustrate the data that permit this comparison for both surface preparations and fatigue stress ratios.

In Figure 25, it is observed that for R=0.1 the curves for the 120W test condition lie above those for the RTW test condition for both surface preparations. This indicates that during fatigue testing, bondline integrity degrades more rapidly at room temperature than at 120 °F. On the other hand, the specimens tested at 120W failed earlier than those tested at RTW. These early 120W failures occurred through the boltholes in the grip area and in the 10-11,000 cycle range. Had the grip failures not occurred, the slower rates of bondline degradation indicated by the C-scans might well have produced considerably longer lifetimes for the 120W specimens. The C-scans on these 120W specimens indicated bondline deterioration under both ends of the patch had begun. If the panels were slightly bent, both ends of these patches could be seen to slightly lift off the metal. The more completely degraded RTW specimens all exhibited interfacial failure, the GBS/BR127 specimens between the adhesive and the primer (I_{ap}) and the SS/no-primer specimens between the adhesive and the metal (I_{ma}).

In Figure 26, it is seen that for R=0.5 the curves for the 120W specimens also lie above the RTW curves for both surface preparations. This again indicates that degradation of the bondline integrity proceeds more rapidly under RTW test conditions than under 120W test conditions. In all four specimens represented by these curves, there was a significant amount of interfacial failure. In the case of the GBS/BR127 specimens, the debonding occurred along the adhesive-primer interface (I_{ap}) while in the case of the SS/no-primer specimens, it occurred along the adhesive-metal interface (I_{ma}).

The differences described above between the RT-wet and 120 °F-wet fatigue behavior may be attributed to a reduction in the residual bondline stress that results from a coefficient of thermal expansion mismatch between the aluminum and the composite patch.

In summary, for both stress ratios and for both surface preparations, the RTW test condition appeared to be more degrading than the 120W test condition.

5.3.2.4 *Effect of Stress Ratio on Fatigue Performance*

As described in Section 4.5, the fatigue tests consisted of tension-tension loading with a minimum/maximum stress ratio of either 0.1 or 0.5. The lower ratio represents the more severe condition because the specimen is being subjected to a larger stress fluctuation during each cycle. In the extreme case of R=1.0 there would be no cyclic stress at all, only a constant unchanging stress level. In other words, one would have a creep or stress-rupture test rather than a fatigue test. As would be expected from this consideration, the results discussed below demonstrate that specimens tested at R=0.5 exhibit significantly less bond integrity degradation than those tested at R=0.1 in nearly every case.

There are six combinations of processing/test conditions for which the two different stress ratios can be compared. These include two test temperatures (room temperature and 120 °F), two aging conditions (dry and wet), and two surface preparations (GBS/BR127 and SS/no-primer). Figures 27 and 28 illustrate the comparative effect of stress ratio on retention of bondline integrity during fatigue testing. The following paragraphs each focus on a single surface preparation and compare the behavior of the specimens tested at R=0.1 to that of specimens tested at R= 0.5.

GBS/BR127 Surface Preparation

Figure 27 contains three pairs of curves for specimens with the GBS/BR127 surface preparation. Each pair contrasts the retention of bondline integrity for the two different fatigue ratios at a single test condition. The two uppermost curves represent the RTD test condition. It is evident that for R=0.5 there is hardly any change in bondline integrity, even out to 120,000 cycles. For R=0.1, on the other hand, the bondline integrity has dropped by 10 percent after 40,000 cycles. Since for this test condition the specimen tested at R=0.5 didn't fail, and the specimens tested at R=0.1 failed predominantly in the metal, no comparison of bondline failure mode could be obtained.

For the RTW test condition, the two lowermost curves in Figure 27 compare the effect of stress ratio. It is evident that for both stress ratios, the bondline integrity deteriorates rapidly during the first 20,000 cycles. The difference is that for R=0.5, the bondline integrity levels off at about 40 percent of its initial value while for R=0.1, the bondline integrity continues to deteriorate. In both cases, the bondline deterioration consists of debonding along the adhesive-primer interface (I_{ap}).

For the 120W test condition, the two central curves compare the effects of R. At this test condition the curve for R=0.1 lies above that for R=0.5. Both exhibited debonding of the patch along the adhesive-primer interface (I_{ap}) in addition to failure through the bolt-holes.

In summary, for the GBS/BR127 specimen, a stress ratio of 0.5 resulted in less significant bondline deterioration than a stress ratio of 0.1 for two of the three conditions, and in longer fatigue life, regardless of the failure mode, in all three test conditions.

54

<u>SS/No-primer Surface Preparation</u>

Figure 28 presents the same data for the SS/no-primer surface preparation that Figure 27 did for the GBS/BR127 specimens. For the RTD condition, it is apparent that the 0.5 stress ratio condition leads to a much lower rate of deterioration in bondline integrity than the 0.1 stress ratio, although for both cases the deterioration that does occur is at the adhesive-metal interface (I_{ma}).

For the RTW condition, both stress ratios cause rapid and severe degradation of bondline integrity along the adhesive-metal interface. For R=0.5 however, the degree of degradation levels off at around 80 percent while for R=0.1, it continues.

For the 120W condition, the curves clearly show that the 0.1 stress ratio produced more rapid degradation of bondline integrity and earlier failure than the 0.5 stress ratio.

In summary, for the SS/no-primer surface preparation, the 0.1 stress ratio causes more bondline degradation than the 0.5 stress ratio and shorter fatigue life regardless of failure mode.

5.4   CORRELATION OF TEST RESULTS

One objective of this program was to determine if the tension-tension fatigue results could be correlated to the wedge crack-propagation results. The wedge test results effectively discriminated between the surface preparation that was known to be resistant to environmental degradation, and the one that was believed to have inferior environmental durability. This discrimination occurred both in the crack length that developed, as well as in the locus of failure, which was along the interface between the adhesive and the metal in the inferior surface preparation and cohesive in the good surface preparation.

In the fatigue tests, the two different surface preparations could be compared on the basis of their relative number of cycles to failure, failure mode, and either rate or degree of bondline integrity degradation as indicated by C-scan signatures. By each criteria, the GBS/BR127 surface preparation appears superior to the SS/no-primer surface preparation.

The fatigue lifetime of the GBS/BR127 specimens was equivalent to or exceeded that of the SS/no-primer specimens for each test condition. The failure mode of the SS/no-primer specimens was predominantly at the metal-adhesive interface, even for the dry unaged specimens, indicating that this was the least durable part of the adhesive joint. The failure mode of the GBS/BR127 specimens, on the other hand, was not along the metal interface. It was predominantly along the adhesive-primer interface in the wet-aged specimens and in the metal outside the adhesive bond on the dry unaged specimens.

The rate of bondline integrity degradation can be estimated by measuring the slope of the curves in Figures 24 through 26. Table 8 lists the slopes of these curves over the first 10,000 fatigue cycles. It is evident that the slopes of the SS/no-primer curves are greater than those of the GBS/BR127 curves, indicating more rapid loss of bondline integrity over the 0-10,000 cycle range. Likewise, if the percent of initial bondline integrity remaining at the time of the specimen failure is examined, it is evident from the curves in Figures 24 through 26 that, for the same test conditions, the GBS/BR127 specimens were much less degraded than the SS/no-primer specimens.

In summary, there definitely does appear to be a correlation between the resistance to environmental degradation observed in wedge testing and that occurring in the type of fatigue testing conducted in this investigation.

Table 8. Rate of Degradation of Bondline Integrity (1)

Test Condition (2)	Surface Preparation	
	GBS/BR127	SS/No-primer
RT Dry/R=0.1	-0.28	-1.61
RT Dry/R=0.5	~0	~0
RT Wet/R=0.1	-2.04	-3.11
RT Wet/R=0.5	-3.5	-8.0
120°F Wet/R=0.1	-0.5	-3.6
120°F Wet/R=0.5	-1.6	-1.4

(1) Numbers represent slopes of curves appearing in Figures 24 through 28. Units are [percent loss of bondline integrity per 1000 cycles].

(2) R=stress ratio during fatigue testing.

SECTION 6

CONCLUSIONS

1. Wet-aging, with no applied stress during aging, did not result in any change in the C-scan signature of the patched specimens. No comparison of bond strength between aged and unaged samples prior to fatigue loading was made.

2. Based on the progressive changes in C-scan signatures with increasing numbers of fatigue cycles, the results clearly demonstrated that the GBS/BR127 surface preparation is more durable than the SS/no-primer surface preparation. This difference in durability was observed at all test conditions.

3. In addition to the differences in durability exhibited by the C-scans, there was a consistent difference in failure mode between the specimens with a GBS/BR127 and those with a SS/no-primer surface preparation. Those with the SS/no-primer treatment failed at the interface between the metal and the adhesive while those with a GBS/BR127 treatment failed either in the metal away from the patch or along the interface between the adhesive and the primer.

4. Specimens that were wet-aged prior to fatigue testing exhibited much more rapid degradation of bondline integrity during fatigue cycling, as indicated by C-scan signatures, than those that were tested in the dry condition.

5. In the case of the GBS/BR127 surface preparation, wet-aging prior to fatigue cycling caused a change in fatigue failure mode. While the specimens tested in the dry condition failed in the metal, either away from or at the end of the patch, those wet-aged before fatigue testing failed along the adhesive-primer interface. In the case of the SS/no-primer surface preparation, there was significant evidence of interfacial failure along the metal-adhesive interface in the dry condition tests and predominant failure along this interface in the wet-aged specimens.

6. For both surface preparations and for both fatigue stress ratios, the RT-wet test condition appeared to be more degrading than the 120°F-wet test condition. The C-scan signatures for the 120W tests indicated significantly slower rates of bondline degradation than for the RTW tests.

7. Specimens tested at a stress ratio of R=0.5, exhibit less degradation of bondline integrity, as indicated by C-scan signatures, than those tested at a ratio of R=0.1, in five of six cases where comparisons could be made. The 0.5 stress ratio resulted in longer fatigue life than the 0.1 stress ratio for all cases and regardless of the failure mode.

8. For the extreme cases of good and poor surface preparations examined here, there was a lot of correlation between the behavior of wedge crack-propagation specimens and the behavior of the fatigue specimens.

SECTION 7
REFERENCES

1.   Schweinberg, Wm., Engineering Task Description, August 1996.

2.   Kuhbander, R. J., "Grit-Blast/Silane Aluminum Surface Preparation for Structural Adhesive Bonding," UDR-TR-94-153, October 1994.

3.   Baker, A. A., "Crack Patching: Experimental Studies, Practical Applications," in Bonded Repair of Aircraft Structures, ed. by A. A. Baker and R. Jones, Martinus Nijhoff, Dordrecht, 1988.

4.   Askins, D. R., "Composite Repair of Cracked Aluminum Structure," UDR-TR-97-98, June 1997.

5.   Popov, E. P., Mechanics of Materials, Prentice-Hall, Englewood Cliffs, NJ, 1982.

6.   Schweinberg, W., Private Communication, July 1998.

APPENDIX A

REPAIR PATCH DESIGN CALCULATIONS

A.1 Calculation of Patch Thickness for 0.125-inch Thick Substrate Panel

The target composite patch-to-substrate aluminum stiffness ratio was 1.2. The patch thickness required to achieve this ratio was determined by means of the calculations shown below. The actual stiffness ratio delivered by the 11-ply patch was 1.23.

For a target stiffness ratio of 1.2,

$$t_{cp}E_{cp} = 1.2t_{al}E_{al} \qquad (A1)$$

where: t_{cp} = thickness of composite patch
t_{al} = thickness of aluminum (0.125 inch)
E_{cp} = modulus of composite patch (28 x 10^6 psi)[1]
E_{al} = modulus of aluminum (10 x 10^6 psi)[1]

Inserting numerical values into (A1) gives,

$$t_{cp} = \frac{(1.2)(0.125\text{-inch})(10 \times 10^6 \text{ psi})}{(28 \times 10^6 \text{ psi})} = 0.0536 \text{ inch} \qquad (A2)$$

For a nominal ply thickness of 0.005 inch, the calculated composite thickness requires 10.72 plies to deliver the target stiffness ratio of 1.2. This was consequently rounded off to 11 plies, which gives t_{cp} a value of 0.055 inch and produces an actual stiffness ratio of 1.23.

---

[1]From Reference 3.

A.2   Calculation of Overall Patch Length

The determination of the overall patch length first requires the calculation of a value for the load transfer length of the patch, and secondly the determination of the taper length on each end of the patch. In this investigation, it was determined by WR-ALC/TIEDD that the length of the constant thickness portion of the patch should be double the length suggested by Baker ($12/\beta$ rather than $6/\beta$). Baker's procedure for determining total patch length [Ref. 3] then combines these two quantities as shown in the equation below to obtain a total overall patch length.

$$\text{Total overall patch length} = 2L_R = 2(12/\beta) + 2(\text{taper length}) \qquad (A3)$$
(see equation 6.25 in Ref. 3)

where: L_R = half length of patch (length on each side of crack)
β = load transfer length on each side of crack

The value for β is determined from the following equation:

$$\beta^2 = \frac{G_A}{t_A}\left[\frac{1}{E_{al}t_{al}} + \frac{1}{E_{cp}t_{cp}}\right] \qquad \text{(see equation 6.1c in Ref. 3)} \qquad (A4)$$

where: G_A = shear modulus of adhesive between patch and aluminum substrate (10^5 psi)
t_A = thickness of adhesive bondline (0.006 inch)
E_{al}, t_{al}, E_{cp}, and t_{cp} are as defined in A.1 (t_{cp} = 0.055 inch)

Plugging numerical values into equation (A4) gives, $\beta = 4.91$ inches^{-1}

The taper length is determined by multiplying the ply drop off length by the number of drop offs. Since there are a total of 11 plies, there are 10 drop offs, each equal to 10 times the thickness of one ply. Thus,

$$\text{taper length (on one end of patch)} = 10(0.005 \text{ inch})(10) = 0.5 \text{ inch} \qquad (A5)$$

Inserting numerical values for β and the taper length into (A3) gives,

Total overall patch length = 24/4.91 + 2(0.5) = 5.89 inches. This value was rounded up to 5.90 inches for the final overall patch length and the ply drop off criteria then dictated that the individual ply lengths ranged from 4.90 to 5.90 inches (see Figure 2, Section 3.2).

APPENDIX B

RATIONALE FOR NOT CONSTRAINING SPECIMEN DURING ADHESIVE CURE

One of the issues that arose during the initial discussions of what the specimen configuration and process procedures should be was whether or not to constrain the panels during bonding so as to prevent or minimize the panel warpage, This normally results from the thermal expansion coefficient mismatches between the aluminum and composite materials. In on-aircraft repairs, the application of heat to a localized area does not result in as much dimensional change in the substrate material as would be expected from thermal expansion considerations alone. The reason for this is that the surrounding structure, not having been heated, has not undergone thermal expansion and thereby acts to restrict the expansion of the localized heated area. This issue was considered from both the practical aspect of how it might be accomplished as well as from the analytical perspective of what the implications of constraint versus freedom to expand were.

The degree of expansion that occurs in an on-aircraft situation is highly variable and depends on a number of factors, including the geometry and stiffness of the surrounding structure and substructure and the degree of curvature of the location being heated. Attempting to simulate this constraint situation in the laboratory becomes largely arbitrary and does not produce a generically realistic correspondence to reality. The two extreme conditions that bracket the real case are: (a) totally unconstrained expansion, which in the case of a laboratory fatigue panel with a boron/epoxy patch on one side, results in a warped specimen (convex on the patch side), and (b) totally constrained expansion, in which the panel warps in the opposite direction (concave to the patch side) because the patch shrinks as it cools while the aluminum substrate simply wants to relax the stresses built up as the result of heating. An arbitrary intermediate point between these two extremes may not have been a very realistic simulation of reality and would not have been simple to accomplish by means of some sort of restraining fixture.

These considerations led us to decide that the better option for fabricating the fatigue panels was not to attempt to constrain them during bonding of the B/Ep patch. Rather, it was felt that the panels should be allowed to warp freely as a result of thermal expansion differences. This would at the very least provide a reproducible and known condition that finite element analysis (FEA) has shown to be an exacting one for the bondline and interface.

APPENDIX C
INDIVIDUAL SPECIMEN WEDGE CRACK-PROPOGATION DATA

Table 4 in Section 5.2 presents a summary of the wedge crack-propagation data generated during this program. Each crack length value shown in Table 4 represents and average value for 10 replicate specimens. In this appendix, the crack length values for each individual specimen is tabulated. In addition, if the crack locus moved to the metal interface, the point at which this first occurred is indicated by (A). If there is no such indication, the failures were cohesive within the adhesive layer. These tables also include the relevant material and process details for the specimens.

Two wedge panels were made for each surface preparation investigated. One was made at the beginning of the panel fabrication sequence and a second was made midway or near the end of the sequence so as to establish that the process remained consistent from start to finish.

Table C1. Wedge Crack-Propagation Data for Specimens Made With Grit-Blast Silane Surface Treatment

Panel No: GBS-127-1 & GBS-127-2	Surface Preparation: Grit-Blast Silane
Adherend Material: 7075T6Bare	Exposure Conditions: 120 °F, 95-100% RH
Primer: BR127	Primer Thickness: 0.0001-0.0002 inch
Adhesive: 1 Ply, AF163-2, 0.085 lb/ft²	

Processing Details:
    Surface Preparation: Standard GBS Conditions [Ref. 2]
    Primer Cure: Standard manufacturer's recommended cure schedule
        (see Section 3.4).
    Adhesive Cure: 1 hour at 121 °C (250 °F) under 356-406 mm (14-16 inches) Hg

Spec. No.	Initial Crack Length (in)	Cumulative Growth (in)						Total Crack Length (in)
		1 hr	4 hrs	8 hrs	24 hrs	7 days	30 days	
1-1	1.38	0.03	0.03	0.03	0.03	0.07	0.10	1.48
1-2	1.32	0.06	0.06	0.06	0.08	0.10	0.10	1.42
1-3	1.31	0.05	0.05	0.05	0.07	0.10	0.13	1.44
1-4	1.33	0.02	0.03	0.03	0.05	0.08	0.11	1.44
1-5	1.35	0.01	0.02	0.02	0.03	0.04	0.08	1.43
2-1	1.23	0.06	0.08	0.08	0.11	0.18	0.27	1.50
2-2	1.27	0.07	0.09	0.09	0.11	0.17	0.26	1.53
2-3	1.31	0.04	0.05	0.05	0.07	0.10	0.17	1.48
2-4	1.29	0.04	0.04	0.04	0.06	0.09	0.13	1.42
2-5	1.30	0.05	0.06	0.06	0.07	0.11	0.14	1.44
Avg.	1.31	0.04	0.05	0.05	0.07	0.10	0.15	1.46

Table C2. Wedge Crack-Propagation Data for Specimens Made with Scuff-Sand Surface Treatment

Panel No: SS-1 & SS-2	Surface Preparation: Scuff-Sand
Adherend Material: 7075T6Bare	Exposure Conditions: 120 °F, 95-100% RH
Primer: None	Primer Thickness: No primer applied
Adhesive: 1 Ply, AF163-2, 0.085 lb/ft^2	

Processing Details:
   Surface Preparation: Mechanical abrasion with Scotchbrite
   Primer Cure: No primer was applied
   Adhesive Cure: 1 hour at 121 °C (250 °F) under 356-406 mm (14-16 inches) Hg
               vacuum (see Section 3.5)

Spec. No.	Initial Crack Length (in)	Cumulative Growth (in)						Total Crack Length (in)
		1 hr	4 hrs	8 hrs	24 hrs	7 days	30 days	
1-1	1.25	0.13 (A)	0.37	0.47	0.47	0.53	0.63	1.88
1-2	1.19	0.16 (A)	0.36	0.43	0.50	0.55	0.68	1.87
1-3	1.23	0.23	0.41 (A)	0.49	0.56	0.59	0.72	1.95
1-4	1.31	0.26 (A)	0.53	0.62	0.67	0.71	0.82	2.13
1-5	1.20	0.27 (A)	0.42	0.51	0.58	0.61	0.74	1.94
2-1	1.15	0.17 (A)	0.39	0.50	0.56	0.68	0.80	1.95
2-2	1.22	0.37 (A)	0.44	0.49	0.56	0.60	0.70	1.92
2-3	1.19	0.36 (A)	0.53	0.64	0.71	0.75	0.86	2.05
2-4	1.21	0.33 (A)	0.47	0.57	0.73	0.83	0.98	2.19
2-5	1.18	0.27 (A)	0.36	0.48	0.61	0.67	0.83	2.01
Avg.	1.21	0.26	0.43	0.52	0.59	0.65	0.78	1.99

APPENDIX D

SCUFF-SAND SURFACE PREPARATION PROCEDURE

The scuff-sand surface preparation is a simple procedure consisting of mechanical abrasion followed by cleaning. The two steps in the procedure are described below:

1. Scrub the surface of the aluminum adherend with Scotch-Brite pad and methylethylketone (MEK).

2. Thoroughly clean the scrubbed surface with MEK and unpigmented/ unscented tissues (i.e., KimWipes). Wipe from center to edge of the surface until NO contamination (black marks or streaks) are evident on the tissues.

LIST OF SYMBOLS, ABBREVIATIONS, AND ACRONYMS

Abbreviation	Definitions
AFRL	Air Force Research Laboratory
ASTM	American Society for Testing and Materials
B/Ep	Boron/epoxy
EPA	Environmental Protection Agency
ETW	Elevated Temperature Wet
FEA	Finite Element Analysis
GBS	Grit-Blast Silane
MEK	Methylethylketone
NDI	Nondestructive Inspection
R	Stress Ratio
r	Least-Squares Correlation Coefficient
RT	Room Temperature
RTD	Room Temperature Dry
RTW	Room Temperature Wet
SS	Scuff-Sand
T.O.	Technical Order
UDRI	University of Dayton Research Institute
WPAFB	Wright-Patterson Air Force Base
WR-ALC	Warner-Robins Air Logistics Center